Crustal flow in Tibet: geophysical evidence for the physical state of Tibetan lithosphere, and inferred patterns of active flow

S. L. KLEMPERER

Department of Geophysics, Stanford University, Stanford, CA 94305-2215, USA (e-mail: sklemp@stanford.edu)

Abstract: Many seismic and magnetotelluric experiments within Tibet provide proxies for lithospheric temperature and lithology, and hence rheology. Most data have been collected between *c.* 88°E and 95°E in a corridor around the Lhasa–Golmud highway, but newer experiments in western Tibet, and inversions of seismic data utilizing wave-paths transiting the Tibetan Plateau, support a substantial uniformity of properties broadly parallel to the principal Cenozoic and Mesozoic sutures, and perpendicular to the modern NNE convergence direction. These data require unusually weak zones in the crust at different depths throughout Tibet at the present day. In southern Tibet these weak zones are in the upper crust of the Tethyan Himalaya, the middle crust in the southern Lhasa terrane, and the middle and lower crust in the northern Lhasa terrane. In northern Tibet, north of the Banggong–Nujiang suture, the middle and probably the lower crust of both the Qiangtang and Songpan–Ganzi terranes are unusually weak. The Indian uppermost mantle is cold and seismogenic beneath the Tethyan Himalaya and the southernmost Lhasa terrane, but is probably overlain by a northward thickening zone of Asian mantle beneath the northern Lhasa terrane. Beneath northern Tibet the upper mantle has not been replaced by subducting Indian and Asian lithospheres, and is warmer than to the south. These inferred vertical strength profiles all have minima in the crust, thereby permitting, though not actually requiring, some form of channelized flow at the present day. Using the simplest parameterization of channel-flow models, I infer that a Poiseuille-type flow (flow between stationary boundaries) parallel to India–Asia convergence is occurring throughout much of southern Tibet, and a combination of Couette (top-driven, between moving boundaries) and Poiseuille lithospheric flow, perpendicular to lithospheric shortening, is active in northern Tibet. Explicit channel-flow models that successfully replicate much of the large-scale geophysical behaviour of Tibet need refinement and additional model complexity to capture the full details of the temporal and spatial variation of the India–Asia collision.

'Only fools, or unusually insightful individuals not yet recognized to be ahead of their time, would doubt that the warmth of the lower crust in regions of extension makes decoupling of upper crust and upper mantle more likely there than in other settings. Thus, the real challenge to understanding how such decoupling or coupling occurs will require study of regions of intracontinental crustal shortening' (Molnar 2000).

Lateral strain variations, and vertical strain and strength profiles in Tibet

Tibet forms the largest and highest plateau on Earth today. Two extreme and opposed views of the mechanism(s) responsible for regional uplift and accommodation of shortening are that: (1) discrete tectonic blocks, internally relatively undeformed, are being expelled eastward between lithospheric strike-slip faults (e.g. Tapponnier *et al.* 1982, 2001); and (2) deformation is essentially continuous, with diffuse deformation of the crust and upper mantle over broad areas (e.g. Dewey & Burke 1973; England & Houseman 1986; England & Molnar 1997; Shen *et al.* 2001), in addition to the convergence taken up at the plateau margins. With the increasing availability of global-positioning data from Tibet and adjacent regions, both in number of sites (now exceeding 500: Zhang *et al.* 2004) and length of their time series (up to nine years: Chen *et al.* 2004), the extreme model of coherent blocks separated by narrow fault zones along which most deformation is localized seems a less plausible description of the active deformation of Tibet. At the Earth's surface there is a continuously varying surface strain field across Tibet when observed at scales of $\geq$100 km (Wang *et al.* 2001; Zhang *et al.* 2004). The major active strike-slip faults such as the Kunlun and Jiali faults (Fig. 1) have motions *c.* 10 mm a^{-1} and separate internally deforming blocks in which about two-thirds of the total 25 mm a^{-1} eastward extrusion of Tibet is accommodated by smaller normal faults and conjugate strike-slip faults (Taylor *et al.* 2003; Chen *et al.* 2004; Zhang *et al.* 2004).

In contrast, vertical strength and strain profiles in Tibetan lithosphere cannot be directly measured, and so remain less certain and more contentious.

From: LAW, R. D., SEARLE, M. P. & GODIN, L. (eds) *Channel Flow, Ductile Extrusion and Exhumation in Continental Collision Zones*. Geological Society, London, Special Publications, **268**, 39–70.
0305-8719/06/$15.00

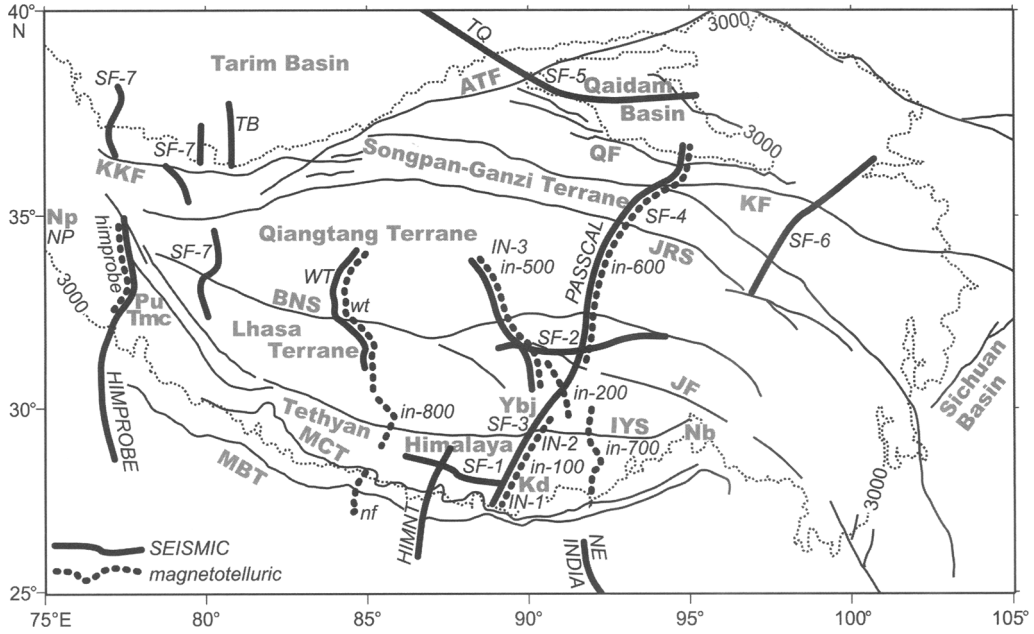

Fig. 1. Location map of main geophysical experiments referred to in this paper. Heavy black lines and upper-case italicized names are generalized location of seismic experiments; heavy dotted lines and lower-case italicized names are magnetotelluric profiles; thin lines are major sutures and faults; thin dotted line is the 3000 m contour. Faults: KKF, Karakax fault; ATF, Altyn Tagh fault; QF, Qaidam Border fault; KF, Kunlun fault; JRS, Jinsha River suture; BNS, Banggong–Nujiang suture; JF, Jiali fault; IYS, Indus–Yarlung suture; MCT, Main Central thrust; MBT, Main Boundary thrust. Himalayan syntaxes: Np, Nanga Parbat; Nb, Namche Barwar. Representative geothermal areas: Ybj, Yangbajain graben in Yadong-Gulu rift; Pu, Puga. Representative north Himalayan gneiss domes: Kd, Kangmar dome; Tmc, Tso Morari complex. Profile names (and selected references): seismic, INDEPTH, IN-1 (Zhao *et al.* 1993; Makovsky *et al.* 1996), IN-2 (Nelson *et al.* 1996; Kind *et al.* 1996; Alsdorf *et al.* 1998*b*; Makovsky & Klemperer 1999), IN-3 (Zhao *et al.* 2001; Ross *et al.* 2004; Huang *et al.* 2000; Rapine *et al.* 2003; Tilmann *et al.* 2003); Sino-French, SF-1 (Hirn *et al.* 1984*a*), SF-2 (Zhang & Klemperer 2005), SF-3 (Hirn *et al.* 1995; Galvé *et al.* 2002*b*), SF-4 (Herquel *et al.* 1995; Vergne *et al.* 2003), SF-5 (Wittlinger *et al.* 1998), SF-6 (Galvé *et al.* 2002*a*; Vergne *et al.* 2003), SF-7 (Wittlinger *et al.* 2004); PASSCAL (McNamara *et al.* 1994, 1995, 1997; Rodgers & Schwartz 1998; Sherrington *et al.* 2004); WT, West Tibet (Kong *et al.* 1996); TB, Tarim basin (Gao *et al.* 2000; Kao *et al.* 2001); NP, Nanga Parbat (Meltzer *et al.* 2001); HIMPROBE (Rai *et al.* 2006); TQ, Tarim-Qaidam (Zhao *et al.* 2006); HIMNT, Himalaya–Nepal–Tibet experiment (Schulte-Pelkum *et al.* 2005); NE INDIA (Mitra *et al.* 2005). Near-vertical reflection profiles are IN-1, IN-2 and locally along IN-3, TB and HIMPROBE; controlled-source wide-angle profiles are SF-1, SF-2, SF-3, SF-6, IN-1, IN-2, IN-3, WT and TQ; teleseismic recording experiments (typically for tomography, receiver-function, shear-wave-splitting, and waveform inversions) are PASSCAL, IN-2, IN-3, SF-3, SF-4, SF-5, SF-6, SF-7, TB, NP, HIMPROBE, HIMNT and NE INDIA. Magnetotelluric profiles: INDEPTH, in-100, in-200 (Chen *et al.* 1996), in-500 (Wei *et al.* 2001), in-600 (Unsworth *et al.* 2004), in-700 (Spratt *et al.* 2005), in-800 (Unsworth *et al.* 2005); himprobe (Gokarn *et al.* 2002); nf, Nepal–French (Lemonnier *et al.* 1999); wt, West Tibet (Kong *et al.* 1996).

Opposing views are that the entire lithosphere deforms homogeneously ('vertical coherent deformation') (e.g. England & Houseman 1986; England & Molnar 1997; Flesch *et al.* 2005), or that deformation is dominated by a more rapid ductile flow in the middle and/or lower crust above a stronger upper mantle ('channel flow') (e.g. Zhao & Morgan 1987; Bird 1991; Shen *et al.* 2001; Beaumont *et al.* 2004). The depth extent of such channelized flow – middle crust, lower crust, or both – depends critically on the actual strength profile. These opposing views have recently been conflated with a new controversy about vertical strength profiles for the continental lithosphere. Laboratory experiments have long been used to infer a combined frictional plus ductile behaviour of the lithosphere, with a quartz-dominated strength maximum in the upper-middle crust, and an olivine-dominated strength maximum at the top of the upper mantle (Brace & Kohlstedt 1980). It is also widely held that the greater part of lithospheric strength is in the upper

crust for typical continental thicknesses and heat flow (e.g. Zoback *et al.* 2003). For 25 years discussions of continental rheology have been dominated by the belief that although earthquakes are largely localized in the upper crust and essentially absent from the lower crust, they do occur, though rarely, in the upper mantle (Meissner & Strehlau 1982; Chen & Molnar 1983), leading to the strong upper crust–weak lower crust–strong upper mantle 'jelly-sandwich' model of continental lithosphere. A strength minimum in the middle-lower crust permits channel flow and complete decoupling of the upper crust and upper mantle, but does not require it: boundary forces arising from plate motions could be applied equally at all depths in the lithosphere, leading to vertically coherent deformation. However, basal drag due to asthenospheric flow is applied to the mantle lithosphere, and body forces due to topographic loads are applied to the crust, and so these will be transmitted upwards or downwards only to the extent that the upper crust is mechanically coupled to the mantle (Flesch *et al.* 2005). An opposing view of continental strength profiles arises from a re-evaluation of the focal depths of supposed upper-mantle earthquakes that places many of these in the lower crust (Maggi *et al.* 2000) leading some to argue that the lower crust is typically stronger than the upper mantle (Jackson 2003; though see Burov & Watts (2006) for counter-arguments). In this case the lack of a broad strength minimum throughout the lower crust must greatly inhibit channel flow, the timescale of which varies inversely with the cube of the layer thickness in which such flow is occurring (for a Newtonian fluid) (Kusznir & Matthews 1988). Even with a weak upper mantle, intracrustal channel flow may still occur as a transient phenomenon due to the introduction of melts or hydrous fluids (McKenzie & Jackson 2002), and widespread lower-crustal flow may occur in conjunction with upper-mantle flow if the viscosities of both are low (Jackson 2003). Clearly, the strong dependence of rock strength on both composition and temperature (e.g. Afonso & Ranalli 2004) as well as hydration state and presence of partial melt (e.g. Kirby 1984; Rosenberg & Handy 2005) means the relative strength of lower crust and upper mantle will vary in time and space, and that an evaluation of this relative strength requires detailed knowledge of the lithosphere.

Modes of crustal flow and channel flow

Any viscous or plastic deformation may be regarded as flow. Such flow need not be channelized within the crust or lithosphere – it may affect the entire outer shell, as in the 'thin viscous sheet' model applied to Tibet by England & Houseman (1986) and England & Molnar (1997), or in the 'vertically coherent deformation' style inferred for Tibet from seismic and geodetic data by Silver (1996) and Flesch *et al.* (2005). In these models, channelized flow is precluded.

In contrast, channel flow as used in this paper refers to any flow in which a viscosity minimum at some depth strongly localizes horizontal material flow and partially or totally decouples flow at different depths (e.g. for Tibet, models of Zhao & Morgan 1987; Bird 1991; Royden 1996; Royden *et al.* 1997; Beaumont *et al.* 2004). Although it is possible to model channel flow with free or partly free boundary conditions (McKenzie *et al.* 2000; McKenzie & Jackson 2002) such models are only now being applied to Tibet (Bendick 2004). The simplest numerical models have explicit channel boundaries with imposed velocity and position conditions. Two end-members are Poiseuille flow (or pipe flow), an extrusion between stationary boundaries in which the induced pressure gradient produces the highest velocities in the centre of the channel (Fig. 2a), and Couette flow, in which shear across the channel produces the highest velocities at the top or base of the channel (Fig. 2b).

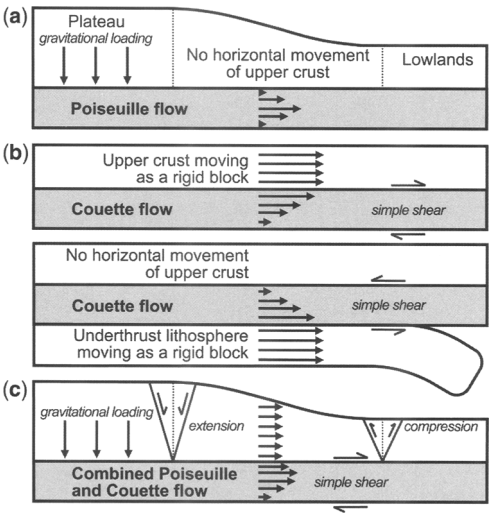

Fig. 2. Modes of channel flow with imposed rigid boundary conditions. Columns of arrows represent relative horizontal velocities. Shaded zones are low-viscosity and undergoing channel flow. No vertical scale is implied; the flowing layer may be all or part of the middle and/or lower crust and/or upper mantle. (**a**) Poiseuille flow (channel flow between stationary rigid boundaries) driven by a pressure gradient. (**b**) Couette flow (channel flow between moving rigid boundaries) driven by upper-crustal extrusion (above) or lithospheric underthrusting (below). (**c**) Combined Poiseuille and Couette flow.

These conceptually useful mathematical simplifications allow approximation of important parameters such as viscosity and channel thickness, but cannot be exact descriptions for Tibetan (or any other mid-lower crustal) flow. Pure Poiseuille flow has been used to model the gentle slopes of the eastern plateau margin (Clark & Royden 2000), and an analogous form of flow emerges naturally in numerous Tibetan deformational models (e.g. Bird 1991; Royden 1996; Royden *et al.* 1997; Shen *et al.* 2001) as a low-viscosity channel within or at the base of the crust. Such models incorporate depth-dependent lower-crustal strength (Royden *et al.* 1997; Shen *et al.* 2001) or thermal weakening (Beaumont *et al.* 2004) that effectively confines flow between boundaries that do not move substantially. In contrast, Couette flow refers to a channelized flow with moving rigid boundaries, for example in which gravitational collapse with outward translation of the upper crust, or underthrusting of cold lithosphere, drives flow in the lower crust by viscous coupling (Beaumont *et al.* 2004) (Fig. 2b). If the entire lower lithosphere is weak, then in this form of flow the entire lithosphere shares the same sense of motion, with velocity decreasing downwards. In recent discussions of Tibetan geodynamics, 'channel flow' has typically been used to describe deformation with Poiseuille (Fig. 2a) or hybrid Poiseuille–Couette characteristics (Fig. 2c).

Independent of numerical models, the concepts of channel flow have been applied to both the Himalaya and Tibet at multiple scales. At a subregional scale, in the NW syntaxis of the Himalaya (Nanga Parbat, Np in Fig. 1), observations of simultaneous high-grade metamorphism, anatexis and rapid denudation led to the recognition of local feedbacks between tectonic and surface processes, and to the 'tectonic aneurysm' model (Zeitler *et al.* 2001) in which large-magnitude river incision focuses deformation of weak crust, leading to crustal flow into the region (Koons *et al.* 2002). The very rapid denudation leading to exposure of Quaternary metamorphic and magmatic rocks, coupled with low seismic velocities, high seismic attenuation and shallow microseismicity (Meltzer *et al.* 2001) leaves little doubt that strongly localized crustal flow exists at present beneath Nanga Parbat (Zeitler *et al.* 2001).

Along the main Himalayan front, seminal observations of extrusion of the crystalline Greater Himalayan Sequence (GHS) (southward with respect to the lower-grade Tethyan Himalaya above and Lesser Himalayan Sequence below) were made first in the central (Burchfiel & Royden 1985), then in the western (Searle & Rex 1989) Himalaya, albeit lacking a channel-flow terminology. Grujic *et al.* (1996), working in the eastern Himalaya, were the first to apply the mechanics of Poiseuille and Couette flow to ductile extrusion of the GHS. However, these and the earlier observations may be as compatible with transient ductile extrusion of a single wedge during growth of a critical-taper orogenic thrust belt, as with a long-lasting channel flow requiring continuous material replenishment into the channel at some unknown location north of the exposures of ductilely deformed GHS rocks. As applied to southern Tibet, the 'channel-flow model' typically refers to the concept, first clearly articulated by Nelson *et al.* (1996), that the GHS represents the ongoing extrusion of a fluid middle crust formed as Indian crust subducted northwards beneath the Lhasa terrane heats up, partially melts, and forms a southward-directed return flow driven by the gravitational potential energy of the Tibetan Plateau. In this view the leucogranites exposed within the GHS represent progressively younger, frozen, snapshots of the partially molten mid-crustal layer interpreted from INDEPTH seismic and magnetotelluric (MT) data north of the Indus–Yarlung suture (Brown *et al.* 1996; Makovsky & Klemperer 1999; Li *et al.* 2003). Wu *et al.* (1998) explicitly added to this model the importance of orographic precipitation (the Indian monsoon) to denudationally exhume the return flow to the surface between coaeval slip (Hodges 2006) on the normal-sense South Tibetan Detachment (STD) above and the thrust-sense Main Himalayan Thrust (MHT) or Main Central Thrust (MCT) below. This concept and a broad range of observed Himalayan metamorphic and geochronologic data have been successfully modelled in two dimensions with time-varying, plane-strain, coupled thermal–mechanical finite-element numerical models (Beaumont *et al.* 2004; Jamieson *et al.* 2004) in which sufficient radiogenic self-heating and mantle heat flux exist to create melt-weakening to reduce the channel viscosity to 10^{19} Pa s. The preferred model of Beaumont *et al.* (2004) and Jamieson *et al.* (2004) is successfully tuned to provide dramatically good fits to a wide range of geological observations, but requires some arbitrary forcing functions (e.g. an arbitrary time-variable surface denudation rate to drive the channel exhumation), and grossly simplifies some aspects of geological evolution (e.g. assumes a continuous evolution towards the modern low-angle subduction, in contrast to the widely recognized two-stage evolution of the Himalaya (e.g. Leech *et al.* 2005) in which early steep subduction is terminated by a slab break-off event prior to establishment of the modern low-angle subduction). Though it seems remarkable that the Beaumont *et al.* (2004) model can fit current observations so well given the elements of geological history not contained

in their model, Beaumont *et al.* (2006) do show that their modelled channel flows are not strongly perturbed by mantle processes, thereby mitigating at least one cautionary note. Although arbitrarily complex initial parameters and model specifications allow arbitrarily complex fits, the good fit thus far obtained provides encouragement for the future that more complex models based on a more complete understanding of initial conditions will continue to fit the complete geological history.

At the largest scale, simpler models (lacking thermal–mechanical coupling but tractable in three dimensions) have explored how gravitational potential can drive outward channel flow from the Tibetan Plateau with wavelengths >1000 km to produce marginal surface uplifts of *c.* 2 km, in a tunnelling Poiseuille mode (Royden *et al.* 1997; Clark & Royden 2000; Hodges 2006). In these models the flow is channelized in the vertical domain by a specified and strongly depth-dependent rheology (Shen *et al.* 2001) and confined laterally by resistant (high-viscosity) crustal blocks along Tibet's southern and northern margins (India, Tarim, Qaidam) and locally along the eastern margin (Sichuan Basin) (Clark *et al.* 2005). The absence in eastern Tibet of exposed middle or lower crust (the lack of an analogue to the GHS) is explained by insufficient denudation to exhume the channel. Such 'channel injection' models are further developed by Medvedev & Beaumont (2006).

Whether at the scale of the individual gneiss domes of the Himalayan syntaxes, the GHS along the length of the Himalaya, or the entire Tibetan Plateau, these proposed models may all be termed channel flow. Independent of terminology, a key task for geophysics is to define the spatial variation of relative vertical strength profiles in Tibet, controlled by lithology, temperature and fluid content; and hence to define the relative vertical velocity profiles, controlled by plate-tectonic boundary forces, topographic (gravity) forces, and asthenospheric basal drag forces.

Geophysical data bearing on crustal flow in Tibet

Data sources

It is the aim of this paper to summarize the now large number of geophysical measurements in Tibet that bear on the composition, temperature and fluid content of Tibetan lithosphere. Referencing is of necessity selective: the Georef database contains 4000 articles published since 1990 with 'Tibet' or 'Himalaya' in the title. Twenty years ago a review of geophysical constraints on the deep structure of Tibet (Molnar 1988) was still able to comprehensively reference the entire preceding literature. Many seminal studies discussed by Molnar (1988) are not further reviewed here: it was by then already possible to conclude that Tibetan crust averages 65–70 km in thickness, and that there is marked lateral heterogeneity in the mantle beneath Tibet, with lower shear-wave velocities and higher attenuation defining a warmer mantle beneath northern Tibet that compensate a somewhat thinner crust there than in southern Tibet.

The availability of portable digital recorders enabled a new generation of geophysical experiments in Tibet in the 1990s that continue to the present day, yielding data that in both quality and density exceed that possible in earlier projects. Figure 1 shows the locations of projects discussed in this paper. Acronyms in Figure 1, upper-case for seismic measurements, lower-case for magnetotelluric (MT) profiles, are used in the text to indicate from which data-set particular results were derived. Three collaborations have provided many crucial data reviewed here: (1) the pioneering multidisciplinary 'Sino-French' transect that recorded controlled-source seismic, teleseismic, MT and geothermal data in southern Tibet in 1980–1982, and continued across the entire plateau with a series of teleseismic and wide-angle seismic experiments through the 1990s and 2000s (sometimes utilizing the name 'Lithoscope') (transect locations SF-1 to SF-7 in Fig. 1); (2) the 1991–1992 Sino-US 'PASSCAL' transect that recorded the first broad-band seismic profile across Tibet on 11 seismographs at *c.* 150 km spacing; and (3) the 1992–1998 'INDEPTH' (International Deep Profiling of Tibet and the Himalaya) experiments that recorded the first deep near-vertical reflection profiles on the plateau (IN-1), and have since recorded controlled-source, passive-source (IN-1, -2, -3) and MT data (in-100, -200, -500, -600) in a corridor across the plateau (this transect will continue in 2007 as INDEPTH-4 across the northern boundary of Tibet). Without minimizing the contributions of many other groups, these three international programmes collected data that continue to be reanalysed today, a decade or more after acquisition. All three transects focused their efforts along the NNE-trending Lhasa–Golmud highway and areas accessible from it, at *c.* 88–95°E, leading to a strong concentration of data-sets in eastern Tibet (Fig. 1). However, although reflection and refraction experiments typically obtain data only directly beneath the seismic array, shear-wave splitting and receiver-function observations pertain to a region several tens of kilometres around the recorders (depending on the depth of the anomaly), body-wave tomography and local-seismicity recordings effectively study a region several hundreds of

kilometres around the array, and regional waveform modelling and surface-wave inversions provide measurements integrated over earthquake-to-receiver paths of 10^2–10^3 km that can average properties of the entire plateau, even if recorded on only a single station. Although MT measurements are largely sensitive to structure directly beneath the array, their relative low cost, speed and simplicity have allowed acquisition that spans the plateau from north to south along the INDEPTH transect, and from west to east in southern Tibet (in-100 to in-800, nf and himprobe in Fig. 1). The other fundamentally new datasets that became available in the 1990s were high-resolution topography and moderate-resolution gravity data for the entire plateau. Some newer geophysical transects along the southern margin of Tibet (HIMPROBE, HIMNT, NE India in Fig. 1) are sufficiently recent that their data are not yet fully published.

Topography and gravity: evidence for intra-crustal compensation

The availability since the early 1990s of sub-100 m lateral-resolution topographic data for Tibet has allowed analysis of the wavelengths on which relief is developed. The low relief of the interior of the Tibetan plateau suggests that upper-crustal isostatic compensation acts to level the surface of the plateau, requiring a 'fluid lower-crustal process' – the crust is not strong enough to maintain large topography at the surface or corresponding stresses at depth (Fielding *et al.* 1994). Detailed analysis of short-wavelength flexural rift-flank uplift adjacent to Plio-Pleistocene grabens in Tibet implies a low-viscosity middle and lower crust (Masek *et al.* 1994) such that the crustal viscosity in a 15-km-thick channel would be *c.* 3×10^{20} Pa s. Braitenberg *et al.* (2003) and Jordan & Watts (2005) used a range of forward and inverse techniques to map the spatial variation of elastic thickness (T_e) and to show the interior of the plateau has T_e typically <20 km, whereas the Himalayan foreland has T_e >100 km (more than double older estimates of McKenzie & Fairhead 1997), and the Tarim, Qaidam and Sichuan basins north and east of the plateau have T_e *c.* 50 km. Modelling of T_e has also been used to define an area of lithosphere beneath southern Tibet that can be identified as Indian mantle sufficiently strong that it must subduct rather than undergo internal deformation (Jin *et al.* 1996). Hence Jin *et al.* map out the 'Indian mantle suture' (point at which top of subducting Indian crust intersects Tibetan Moho) and the 'Indian mantle front' (northernmost extent of Indian lithosphere beneath Tibet), at latitudes *c.* 29.5°N and *c.* 33°N along the Lhasa–Golmud highway.

In contrast to the southern and northern margins of Tibet, where Quaternary upper-crustal deformation is occurring as shown by modern seismicity and mapped fault patterns, the eastern margin of the plateau lacks large-scale Quaternary surface shortening (Royden *et al.* 1997). This can be modelled if the lower crust is sufficiently weak (10^{18} Pa s in a 15-km-thick layer) to decouple the upper crust from the upper mantle (Royden *et al.* 1997; Shen *et al.* 2001). The topography of eastern Tibet and its time-evolution are both compatible with outward flow of a weak crust. Clark & Royden (2000) have shown that the more than order-of-magnitude contrast between the steep plateau margin adjacent to the Tarim basin and Sichuan basin, and the low-gradient slope of the NE and SE plateau margins, can be explained by a lower-crustal channel with lateral variations in viscosity. Assuming pure Poiseuille flow in a 15-km-thick channel, they inferred channel viscosities of 10^{21}, 10^{18} and 10^{16} Pa s beneath the steep margins gentle margins, and plateau interior, respectively. Evidence for sequential reorganization of drainage patterns in southeastern Tibet (Clark *et al.* 2004) and rapid late Cenozoic cooling in the southwestern Qinling (Enkelmann *et al.* 2006) as a result of Neogene uplift of the plateau margin is consistent with this model of long-wavelength intra-crustal channel flow. The relative viscosities of Clark & Royden (2000) are important if topography is a proxy for lower-crustal viscosity; their inferred viscosities are less important since they are strongly model-dependent and scale with the cube of the channel thickness. Indeed, the lowest viscosity inferred by Clark & Royden is inherently unlikely because it is hard to reconcile with plausible regional crustal viscosities even if the inferred channel occupies the entire crustal thickness (Hilley *et al.* 2005). Absolute viscosities $<10^{19}$ Pa s probably require a few per cent of *in situ* partial melt (cf. Beaumont *et al.* 2004; Rosenberg & Handy 2005), which should be detectable by magnetotelluric and seismic methods.

Geothermal measurements: evidence for recent magmatism in southern Tibet

Geothermal exploration of the Puga region in NW India (Pu in Fig. 1) measured heat flow >500 mW m^{-2} (Shanker *et al.* 1976), later interpreted as caused by a Quaternary intrusion at the *c.* 7 km depth of local seismicity (Gupta *et al.* 1983). Better known because collected in the framework of a large international project are later Sino-French heat-flow measurements in two lakes in southernmost Tibet (close to Kangmar Dome, Fig. 1) of 91 and 146 mW m^{-2} (Francheteau *et al.* 1984). The large variation over <25 km between the two lakes

requires an anomalous shallow heat source, presumably magmatic, intruded within the past 1 million years at less than *c.* 10 km depth beneath Yamdrok Tso, the northern of the two lakes that extends from 15–50 km south of the Indus–Yarlung suture (Jaupart *et al.* 1985). Additional studies of the 'Himalayan geothermal belt' have documented at least 600 geothermal systems in the Lhasa terrane and northern Tethyan Himalaya, mostly concentrated east of 84°E (Hochstein & Regenauer-Lieb 1998). After correction for convective heat flow, southern Tibet has a regional heat flow of *c.* 82 mW m^{-2} (Wang 2001), equivalent to 'characteristic Basin & Range' heat flow of Lachenbruch & Sass (1977). Regional heat flow in northern Tibet (Qiangtang terrane) is estimated, based on only two measurements, at *c.* 45 mW m^{-2} (Wang 2001), intermediate between the 'Sierra Nevada' and 'Stable reference crust' geotherms of Lachenbruch & Sass (1977). Standard conductive geotherms predict Moho temperatures of *c.* 700°C (i.e. in excess of the pelitic wet solidus (Thompson & Connolly 1995) even in northern Tibet (Wang 2001), due to the ≥60 km crustal thickness. Analogous geotherms predict such extremely high temperatures beneath southern Tibet that the only reasonable scenario is a more isothermal crust than standard, maintained by underthrusting of a relatively cold Indian crust (Wang 2001).

Seismicity cut-off at depth locates brittle–ductile and ductile–brittle transitions

Crustal seismicity, both from teleseismic observations (Molnar & Lyon-Caen 1989; Zhao & Helmberger 1991) and local network studies (PASSCAL: Randall *et al.* 1995; IN-3: Langin *et al.* 2003), is effectively limited to the upper crust. Both teleseismic studies cited, which necessarily focus on larger earthquakes, place 95% of relocated earthquakes above 18 km depth, and both local studies place 95% of located earthquakes above 20 km depth. In particular the Langin *et al.* (2003) study (IN-3) located 267 earthquakes from the Indus–Yarlung suture to the Jinsha River suture, and across 6° of longitude over a nine-month period, thereby providing a comprehensive snapshot of crustal seismicity in east-central Tibet. The downward cut-off of crustal seismicity is widely accepted as marking the brittle–ductile transition at a temperature of 250–450°C (Meissner & Strehlau 1982; Chen & Molnar 1983). By itself, the existence of a ductile lower crust does not demonstrate crust–mantle decoupling, because the mantle could in some circumstances be even weaker than the overlying lower crust (Jackson 2003; Afonso & Ranalli 2004).

However, in contrast to the absence of earthquakes beneath the Tibetan Plateau with well-constrained focal depths of 30–65 km, it is well-documented that earthquakes occur beneath southern Tibet at depths of 70–110 km, some clearly below the Moho. These sub-Moho earthquakes are known from both teleseismic recordings (Molnar & Chen 1983) and temporary local network recordings (PASSCAL: Zhu & Helmberger 1996). Chen & Yang (2004) review evidence for eight subcrustal earthquakes (90–110 km depth) in western Tibet (between the Indus–Yarlung suture and the Altyn Tagh–Karakax fault, are all clearly distinct from the Hindu Kush intra-continental subduction intermediate-depth seismic belt), and for an additional five presumed sub-Moho earthquakes (80–90 km depth) beneath the Tethyan Himalaya and southern Lhasa terrane (all east of 86°E and south of 30°N, hence south of or close to the Indian mantle suture inferred from gravity modelling by Jin *et al.* 1996). A further two earthquakes at 70 km depth in the Himalaya/southeastern Tibet may be in the lower crust or the upper mantle. Some have suggested that all earthquakes in southern Tibet lie above the Moho (Jackson 2003; Mitra *et al.* 2005), pointing to evidence for crustal thicknesses as great as 85–90 km near Lhasa (Yuan *et al.* 1997; Mitra *et al.* 2005), but in doing so ignore significant west–east variations in crustal structure (SF-2: Zhang & Klemperer 2005) including equivalent evidence for thinner crust (70–80 km) closer to the location of the deep earthquakes (IN-2: Yuan *et al.* 1997; Chen & Yang 2004). Hence it seems probable that these deep earthquakes of magnitude 4.3–6.0 are evidence for sub-Moho brittle behaviour in southern Tibet (Chen & Yang 2004), and presumably require temperatures no more than 600–800°C (Chen & Molnar 1983). The evidence for subcrustal earthquakes is even clearer for the eastern Nepal segment of the High and Tethyan Himalaya, where over 100 small earthquakes (magnitude <4.5, recorded on a local network deployed for <18 months) have been located up to 40 km below the Moho (up to 100 km below sea-level) in a joint tomographic/receiver-function inversion (HIMNT: Schulte-Pelkum *et al.* 2005; Monsalve *et al.* 2005, 2006). This evidence for significant strength in the mantle beneath the Himalaya is unsurprising if elastic thicknesses there are indeed of the same order as crustal thickness (Jordan & Watts 2005).

Seismic velocity and crustal thickness: north–south dichotomy of uppermost-mantle velocities but plateau-wide low crustal velocities

Seismic velocities at any depth depend on lithology, temperature and fluid distribution. Low velocities

tend to correlate with higher SiO_2 content (Christensen & Mooney 1995), hence with lower melting point, and hence lower creep strength at any given temperature since the homologous temperature is lower at any given temperature (e.g. McKenzie & Jackson 2002). Seismic velocities decrease with increased temperature (Christensen & Mooney 1995), which weakens rocks. Velocities are also greatly reduced by addition of aqueous (Hyndman & Shearer 1989) or magmatic (Hammond & Humphreys 2000) fluids that also weaken their host rocks (Kirby 1984; Rosenberg and Handy 2005). Crust or mantle with unusually low seismic velocities is therefore weaker than average, and pronounced low-velocity zones relative to material above and below indicate low-strength channels in the lithosphere.

The recognition of marked lateral heterogeneity in the mantle beneath Tibet remains one of the most fundamental and reliable observations bearing on Tibetan geodynamics. Evidence for a warmer upper mantle beneath northern Tibet east of 85°E, as compared to southern Tibet, was first found in strong attenuation of Sn (uppermost mantle shear-wave) (Ni & Barazangi 1983) and lower upper-mantle shear-velocity beneath a thinner crust inferred from Rayleigh-wave-phase velocities (Brandon & Romanowicz 1986). These early studies using seismic stations outside Tibet have been reinforced and extended to include P-wave observations from portable broadband deployments in eastern Tibet by the PASSCAL (McNamara *et al.* 1995, 1997), Sino-French Lithoscope (SF-4: Wittlinger *et al.* 1996) and INDEPTH (IN-3: Tilmann *et al.* 2003) groups. All these datasets show significant differences (McNamara: 3–4%; Tilmann: 2%) between a faster mantle south of approximately the Banggong–Nujiang suture and slower mantle further north, corresponding to a temperature increase of *c.* 200–300°C from south to north (McNamara *et al.* 1997), significantly lower than earlier estimates as high as 500°C (Molnar *et al.* 1993). Noting that all these temporary deployments were located east of 88°E, Dricker & Roecker (2002) use teleseismic SS-S differential traveltimes (that are sensitive to structure to depths of *c.* 300 km) to show that the north–south mantle variability is only pronounced in eastern Tibet. In their model, Tibetan mantle west of 87°E is uniformly faster (colder) than to the east, providing an ongoing disagreement with the Pn tomography of McNamara *et al.* (1997) that shows low uppermost mantle velocities extending west to 80°E, north of the Banggong–Nujiang suture. Unfortunately Pn has not been observed on controlled-source refraction profiles recorded over the Tibetan Plateau due to the great crustal thickness and strong crustal attenuation.

Despite the south–north change in temperature of the lithospheric mantle, lithospheric thickness appears relatively uniform. Kumar *et al.* (2006) use S-to-P receiver functions to map a plateau-wide discontinuity that they identify as the lithosphere–asthenosphere boundary. The base of the Indian lithosphere dips north from *c.* 170 km beneath the Himalaya to *c.* 210 km beneath the Banggong–Nujiang suture; and the base of the Asian lithosphere is nearly horizontal at 170 to 190 km beneath central and northern Tibet (Kumar *et al.* 2006).

Waveform modelling of earthquake phases at regional distances (e.g. so-called Pnl waveforms comprising the P arrival (Pn) followed by the crust-trapped P-SV multiple conversions (PL)) is an effective way to study crustal velocities averaged laterally over hundreds of kilometres. For Tibet, Rodgers & Schwartz (1998) demonstrate that average crustal P-wave velocity (Vp) in the Qiangtang and Lhasa terranes (6.2 and 6.0 km s^{-1}) is significantly less than the global continental average of 6.45 km s^{-1} (Christensen & Mooney 1995). Controlled-source refraction experiments typically provide the best-resolved estimates of Vp (e.g. SF-1: Hirn *et al.* 1984*a*; IN-3: Zhao *et al.* 2001; SF-6: Galvé *et al.* 2002*a*), and further demonstrate that Tibetan crust has unusually low seismic velocity at all depths compared to global averages (Haines *et al.* 2003). Despite the low average Vp, many studies – including receiver-function and related P-waveform modelling methods that detect the amplitude and polarity of Moho and intracrustal conversions – suggest a higher-velocity layer (>7 km s^{-1}) at the base of the crust. This higher-velocity layer is *c.* 12 km thick in the Tethyan Himalaya (SF-1: Hirn *et al.* 1984*a*), *c.* 20 km thick in the southern Lhasa terrane south of 31°N (IN-2: Kind *et al.* 2002), *c.* 10 km beneath the northern Lhasa terrane (PASSCAL: Zhao *et al.* 1996; Owens & Zandt 1997) and southern Qiangtang terrane (IN-3: Zhao *et al.* 2001), and *c.* 20 km thick in the Qiangtang and Songpan–Ganzi terranes (SF-4 and -6: Vergne *et al.* 2002). The presence of this higher-velocity lower-crustal layer means that the upper and middle crust must have even lower velocity for the crustal average to be so low. The high-velocity layer may represent Indian cratonic lower crust: DeCelles *et al.* (2002) offer the provocative hypothesis that 'Greater Indian lower crust' extends beneath Tibet to the Kunlun fault, even if Greater Indian mantle extends no further north than southern Tibet.

Receiver functions provide independent estimates of crustal velocity structure beneath individual stations, e.g. along the INDEPTH-2 transect (Yuan *et al.* 1997) or across the entire plateau along the 1991–1992 Sino-US PASSCAL experiment (Owens & Zandt 1997). These studies

identify a distinct low-velocity zone below 20 km depth in the Lhasa terrane which dies out southward approximately at the Indus–Yarlung suture (IN-2: Kind *et al.* 1996), and confirm the unusually low average-crustal Vp across the entire plateau, as well as suggesting low lower-crustal S-wave velocity (Vs) and correspondingly high Vp/Vs in the northern plateau (PASSCAL: Owens & Zandt 1997; IN-3: Tian *et al.* 2005). A reinterpretation of the PASSCAL results in conjunction with transect SF-4 (Vergne *et al.* 2002) highlights the inherent non-uniqueness of receiver-function inversions (even in the absence of anisotropic or dipping structure) (Ammon *et al.* 1990), and suggests Vp/Vs ratios north of the Banggong–Nujiang suture are normal, with no evidence for widespread partial melting beneath the Qiangtang terrane.

Surface-wave studies integrate over large regions of the crust and are particularly useful for picking out broad trends in crustal velocity (Fig. 3). Early teleseismic surface-wave observations used to document a crustal low-velocity zone throughout Tibet (Chun & Yoshii 1977) have been refined by more detailed observations from the INDEPTH transects that provide distinct averaged velocity–depth profiles for the Qiangtang and the northern Lhasa terranes (IN-3: Rapine *et al.* 2003), and for the Lhasa terrane and Tethyan Himalaya (IN-2: Cotte *et al.* 1999). All the Vs–depth profiles derived from surface-wave inversions for Tibet are significantly low compared to global crustal values (Fig. 3), as expected from the refraction and waveform-modelling Vp results. Additionally it is clear that there is a strong low-velocity channel in the mid-to-lower crust of the Lhasa terrane, placed at 20–40 km depth (IN-3: Rapine *et al.* 2003), 30–50 km (IN-2: Kind *et al.* 1996) or 30–70 km (IN-2: Cotte *et al.* 1999). This channel becomes less pronounced to the north in the Qiangtang terrane because the overall lower-crustal velocity is lower in the Qiangtang than in the Lhasa terrane (Rapine *et al.* 2003). The

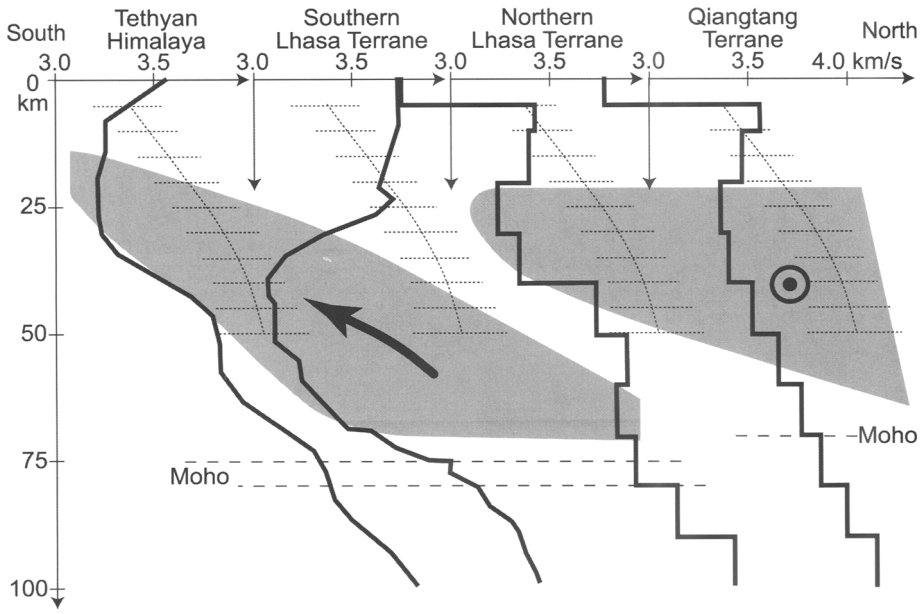

Fig. 3. Surface-wave velocity models along IN-1, -2 and -3. S-wave velocity–depth models of Cotte *et al.* (1999) for the Tethyan Himalaya and southern Lhasa terrane and of Rapine *et al.* (2003) for the northern Lhasa terrane and Qiangtang terrane are shown, each displaced laterally by 1 km s^{-1} from the previous model to allow easy viewing, and to convey a sense of possible continuity of channels of unusually low velocity (grey-shaded regions). Possible dominant flow directions (see text and Fig. 8) are shown by south-directed arrow in southern grey region, and east (out-of-the-page)-directed arrowhead/bullseye in northern grey region. Note possibility of multiple, vertically stacked, independently flowing weak zones, e.g. in northern Lhasa terrane. Dotted curve across and to right of each velocity–depth profile is the mean crustal P-wave velocity of Christensen & Mooney (1995) (only available from 5 to 50 km depth), with horizontal bars showing 1σ from the mean at each depth, scaled by the mean crustal Vp/Vs ratio from Christensen (1996). Note the normal S-velocities in the shallow crust, but S-wave velocities in the low-velocity zones (shaded) that are one to two standard deviations below expected crustal velocities. Dashed lines at 75 km and 80 km in the Lhasa terrane and 70 km in the Qiangtang terrane are likely Moho depths, and highlight the unusually low Sn velocity of the Qiangtang terrane, <4 km s^{-1}.

channel apparently disappears south of the Indus–Yarlung suture (Kind *et al.* 1996) or becomes shallower and is restricted to the upper half of the crust (Cotte *et al.* 1999) (Fig. 3). Yuan *et al.* (1997) suggest that the strongest low-velocity zone is collocated with the seismic bright spots imaged in the Yangbajain graben (IN-2: Brown *et al.* 1996; Makovsky & Klemperer 1999), but also find a possibly analogous feature beneath Lhasa, confirming that the unusual low-velocity structure of southern Tibet is not restricted to the active extensional grabens. Figure 3 shows one possible correlation of different crustal low-velocity zones on the different surface-wave velocity profiles, and my inferred crustal flow directions (see below).

The unusually low crustal Vp (e.g. PASSCAL: Owens & Zandt 1997) can be understood without the necessity of forming Tibet from abnormal crustal compositions if lower (and perhaps also middle) crust has been lost from Tibet by lateral flow (Haines *et al.* 2003), and if there is a small percentage of partial melting in the crust. Even though Vp in Tibet is unusually low, Vp/Vs is variously determined as being normal or high, potentially indicative of low-degree partial melts in the crust (PASSCAL: Owens & Zandt 1997; Rodgers & Schwartz 1998; Vergne *et al.* 2002; IN-3: Tian *et al.* 2005). Locally in the Yangbajain graben of the Lhasa terrane, large S delay times relative to P delay times also seem to require several per cent of melt averaged over the entire crustal thickness (SF-3: Hirn *et al.* 1995). Eclogitization could also reduce measured crustal Vp by placing the Moho above eclogitized lower crust (Haines *et al.* 2003) but may be precluded below the Qiangtang terrane by higher mantle temperatures there. Partial eclogitization is the likely cause of observed unusually high lower-crustal velocities (*c.* 7.4 km s^{-1}) beneath the High Himalaya (HIMNT: Schulte-Pelkum *et al.* 2005) and sub-Moho velocities >8.4 km s^{-1} where the Indian craton is subducting beneath the Tethyan Himalaya (SF-1: Henry *et al.* 1997; Sapin & Hirn 1997). Gravity modelling suggests that eclogitization may continue to develop within the Lhasa terrane lower crust (Cattin *et al.* 2001). Eclogitization might also occur at the northern margin of Tibet where Asian lithosphere may be subducting beneath Tibet (Kind *et al.* 2002; Shi *et al.* 2004). Mafic lower crust seems to be absent north of the Kunlun Fault (SF-4 and -6: Vergne *et al.* 2002) and a 'crust–mantle mix' zone with Vp = 7.3–7.8 km s^{-1} above a mantle velocity of 8.2 km s^{-1} beneath the Altyn Tagh (TQ: Zhao *et al.* 2006) might represent partial eclogitization. Miocene adakitic lavas – globally rare, and thought to represent melting of garnet-bearing sources, hence presumably eclogitized crust – are now known from both the southern Lhasa terrane (Chung *et al.* 2003) and the Songpan–Ganzi terrane (Wang *et al.* 2005).

A fundamental parameter that is well-determined by seismic velocity–depth models is crustal thickness, which varies from 70–80 km in southern Tibet to 60–70 km in northern Tibet (e.g. WT: Kong *et al.* 1996; IN-2, -3, PASSCAL: Kind *et al.* 2002). Some of the earliest controlled-source experiments in Tibet were used to infer large and abrupt Moho offsets beneath the Himalaya, Indus–Yarlung suture and Banggong–Nujiang sutures (SF-1, -2, -3: Hirn *et al.* 1984*a*, *b*). These Moho steps were interpreted using the fan-profiling method in which there are large ambiguities between velocity and structure, and have largely been discounted by subsequent workers (Molnar 1988) and in the light of new data (IN-3: Zhao *et al.* 2001; HIMNT: Schulte-Pelkum *et al.* 2005). However, at the northern margin of Tibet more robust observations of abrupt changes in crustal thickness suggest abrupt changes in crustal rheology. There is good evidence from receiver functions for a large crustal thickness decrease of 10–20 km northwards across the Karakax–Altyn Tagh fault over a lateral distance $\leq$20 km (TB: Kao *et al.* 2001; SF-7: Wittlinger *et al.* 2004). A similar abrupt offset and evidence for southward underthrusting of the Tarim block is also seen across the Altyn Tagh fault where it separates the Tarim and Qaidam basins, from both teleseismic tomography (SF-5: Wittlinger *et al.* 1998) and wide-angle refraction profiling (TQ: Zhao *et al.* 2006). Likewise, Moho offsets are also seen beneath the Qaidam border fault on the PASSCAL, SF-4 and SF-6 profiles (Zhu & Helmberger 1998, Vergne *et al.* 2002), suggesting that a strong Qaidam basin fills the role of the Tarim basin further west, failing to thicken in response to collisional stresses, and marking the northern limit of major Tibetan crustal thickening. This implied strength of the Tarim and Qaidam basins is also seen in their elastic thicknesses, T_e = *c.* 50 km, that significantly exceed values on the Plateau where T_e is typically $<$20 km (Braitenberg *et al.* 2003; Jordan & Watts 2005). From receiver-function profiles along SF-4 and -6 Vergne *et al.* (2002) suggest an additional but potentially much smaller Moho offset below the Jinsha suture. Galvé *et al.* (2002*a*) interpret wide-angle refraction profile SF-6 to show that the largest crustal thickening occurs beneath the Kunlun fault, but a lack of continuous reflection data makes this argument less compelling than the data demonstrating a more abrupt Moho step further north. However, these data (Galvé *et al.* 2002*a*; Vergne *et al.* 2002) arguing for a gradual transition in crustal thickness across northeastern Tibet may correspond to a region of somewhat elevated T_e SE of Qaidam Basin (Jordan & Watts 2005).

Seismic attenuation: evidence for high temperatures and partial melts

Theoretical models and laboratory measurements show an increase of seismic attenuation (or decrease in its inverse, Q) with increased temperature, and particularly with the presence of partial melt. Unusually high attenuation was one of the first geophysical anomalies recognized in Tibet, both in the crust (Ruzaikin *et al.* 1977) and in the upper mantle of northern Tibet (Barazangi & Ni 1982; Ni & Barazangi 1983). More recent waveform modelling studies have refined the degree and extent of these anomalies. The region of strong Sn (upper mantle) attenuation found by Ni & Barazangi (1983) and by McNamara *et al.* (1995, from PASSCAL) also corresponds with unusually strong crustal attenuation, detected by its effect on both Pnl phases (Rodgers & Schwartz 1998, from PASSCAL) and on Lg (trapped post-critical crustal shear-wave) (Fan & Lay 2003, from permanent broadband stations). Both Rodgers & Schwartz (1998) and Fan & Lay (2003) suggest that the high attenuation is a manifestation of widespread partial melting of the crust of northern Tibet. Regional variability in Lg (crustal) Q from 80 to 100°E across Tibet seems no larger than uncertainties in its estimation (Fan & Lay 2002). Southern Tibet has a less attenuating mantle (Ni & Barazangi 1983; McNamara *et al.* 1995) and crust (Fan & Lay 2003) on a regional scale. The strongest attenuation ($Q = c.\ 60$) yet reported from Tibet comes from Lg measurements along the INDEPTH-2 profile in the Yangbajain graben, believed from the lack of frequency dependence to be due to intrinsic attenuation and not to scattering, so presumably due to hydrothermal and magmatic fluids in the upper crust (Xie *et al.* 2004). Q increases southwards to *c.* 100 between the Indus–Yarlung suture and the Kangmar Dome, and to *c.* 300 beneath the High Himalaya (cf. typical values of *c.* 200 in tectonically active western North America and >650 for stable central and eastern North America: Xie *et al.* 2004).

High conductivity zones: evidence for fluids and crustal weakening

Natural-source magnetotelluric (MT) studies in the Sino-French collaboration of the early 1980s demonstrated anomalously high conductivities at shallow depths north and south of the Indus–Yarlung suture zone, both within the Yangbajain graben and outside the Yadong–Gulu rift beneath Yamdrok Tso (Pham *et al.* 1986). The high conductivities were interpreted as magma (Pham *et al.* 1986) because of the correlation with a region of anomalously high heat flow (Francheteau *et al.* 1984; Jaupart *et al.* 1985). A similar correlation exists between very high electrical conductivity and the inferred magmatic source of the highest heat-flow region of NW India (Harinarayana *et al.* 2004). From 1995 to 2001, INDEPTH recorded *c.* 1600 km of broadband and long-period MT data along six profiles that together cross the entire Tibet Plateau in a corridor from 89 to 94°E (Wei *et al.* 2001; Spratt *et al.* 2005), corroborating the older results and providing much new information on the existence of fluids at depth in the crust. Two additional MT transects cross the NW Himalaya at 78°E (himprobe: Gokarn *et al.* 2002) and the Nepal Himalaya at 85°E (nf: Lemonnier *et al.* 1999), the latter continuing into Tibet at the same longitude (in-800: Unsworth *et al.* 2005; wt: Kong *et al.* 1996). Three salient features emerge from the combined data-sets: (1) generally high crustal conductance (integrated conductivity over depth; a far better resolved parameter than the absolute conductivity at any depth) across the entire Tibetan plateau (in-100, -500, -600: Wei *et al.* 2001; Unsworth *et al.* 2004) (Fig. 4); (2) extraordinarily high conductivity below 15 km in the Yangbajain graben, southern Lhasa terrane (in-100 and -200: Li *et al.* 2003), collocated with the seismic bright spots discussed below; and (3) a remarkable continuity of conductivity structure along the entire Himalayan arc from 77 to 92°E (himprobe, nf/in-800, in-100, in-700: Unsworth *et al.* 2005).

Wei *et al.* (2001) show that along the main INDEPTH transect (in-100, -500, -600), from the Himalayan crest to the Kunlun fault, crustal conductance everywhere exceeds typical values for the continents (Fig. 4). North of the Kunlun fault, and south of the STD, conductance declines into the normal range. In the Tethyan Himalaya and southern Lhasa terrane (in-100) the highest conductivities are seen above 30 km depth, and the conductivity anomaly may be confined to the crust; in the northern Lhasa terrane, Qiangtang and Songpan–Ganzi terranes (in-500, -600) the highest conductivities are seen below 30 km depth. In two regions of Tibet conductance is above 10^4 S, exceeding the normal upper bound by more than an order of magnitude (Wei *et al.* 2001): (1) across the Indus–Yarlung suture and in the southern Lhasa terrane (29–30°N, probably associated with the seismic bright spots, and probably confined to the crust; see also Li *et al.* 2003); and (2) locally in the east-central Qiangtang terrane (in-600 but not in-500, at 33–34°N, east along strike from abundant Late Miocene and younger xenolith-bearing volcanic rocks (discussed below; Turner *et al.* 1996; Ding *et al.* 2003), and certainly extending into the upper mantle (see also Unsworth *et al.* 2004). The only sensible explanation for the

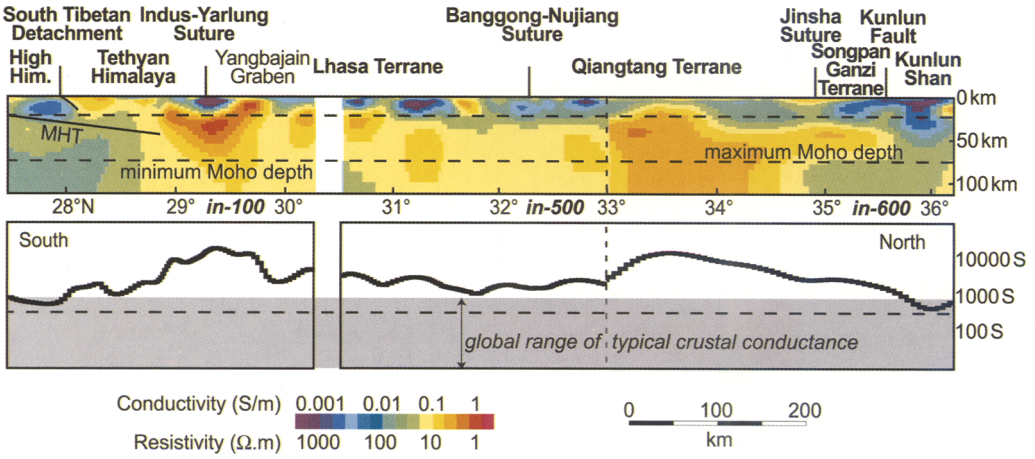

Fig. 4. Lithospheric electrical conductivity of Tibetan Plateau, modified after Wei *et al.* (2001). Top: conductivity models for in-100, -500, -600 (see Fig. 1). Data gap exists at 30.5°N; profiles are offset at 33°N (vertical dashed line) where in-600 is 150 km east of in-500. Horizontal dashed line at 20 km depth emphasizes typically resistive upper crust except in Yangbajain graben and beneath Tethyan Himalaya. Note in-500 lies outside, and northern part of in-100 lies within, the Yangbajain graben thereby showing that high lower-crustal conductivity in the Lhasa terrane is not only related to the Neogene east–west extension. Horizontal dashed line at 70 km depth marks probable minimum Moho depth south of the Banggong–Nujiang suture to emphasize the likely resistive mantle in southern Tibet, and marks the probable maximum crustal thickness north of the Banggong–Nujiang suture and so emphasizes the likely conductive mantle of the Qiangtang terrane. Bottom: total conductance to 100 km depth. Grey-shaded region is range of typical crustal conductance, 10–1000 S and horizontal dashed line is mean Phanerozoic lower-crustal conductance of 400 S (Jones 1992).

high conductance beneath Tibet is interconnected fluid along the grain boundaries of the rock (Wei *et al.* 2001), either partial melt or saline aqueous fluids. Wet rocks and partially molten rocks are both far weaker than their dry counterparts (Kirby 1984; Rosenberg & Handy 2005), thus fluid-rich crust, irrespective of the fluid type, must represent weaker areas able to accommodate deformation by crustal flow. The high observed conductance implies unusually weak crust below 30 km throughout Tibet, with the additional implication of weak upper crust in southern Tibet and weak upper mantle in northern Tibet.

Li *et al.* (2003) provide detailed models for the Yangbajain graben region that satisfy both the high conductivity (Chen *et al.* 1996) and the seismic bright spots (Brown *et al.* 1996; Makovsky & Klemperer 1999). The MT data alone cannot distinguish between end-member models of a >10 km layer of partial melt, or a *c.* 1 km layer containing $>10\%$ saline fluid. The seismic constraints suggest an interpretation combining both likely causes of enhanced conductivity, with *c.* 200 m of *c.* 10% saline fluid above >10 km of *c.* 10% partial melt (Li *et al.* 2003). Gaillard *et al.* (2004) experimentally confirm that hydrous granitic melts can have conductivities as high as those observed beneath the Yangbajain graben, but point out that the presence of crystallizing leucogranites demands some local accumulation of hydrous fluids upon magma solidification, while the occurrence of a large amount of fluids in the middle crust requires that molten granite be present immediately beneath levels that are rich in fluids. Thus a combination of both magmatic and aqueous fluids is required by the joint interpretation of the seismic and MT data and our understanding of the geological evolution of crust-derived melts. The high conductivity beneath the Yangbajain graben, southern Lhasa terrane, collocated with the seismic bright spots, is therefore fully consistent with the Nelson *et al.* (1996) model in which molten analogues of the Miocene High Himalayan leucogranites cause the anomalous conductivity and reflectivity. It is important to note that even though the highest conductivities in southern Tibet are observed in an active hydrothermal area within the Yangbajain graben, abnormal conductance extends outside the graben into unrifted crust: profile in-200 was recorded 80 km (one crustal thickness) NW and SE beyond the limits of the graben, but shows conductivities along its entire length that are anomalous by global standards (Chen *et al.* 1996), as does in-500, also acquired outside the graben system (Wei *et al.* 2001) (Fig. 4). In contrast, the seismic bright spots are

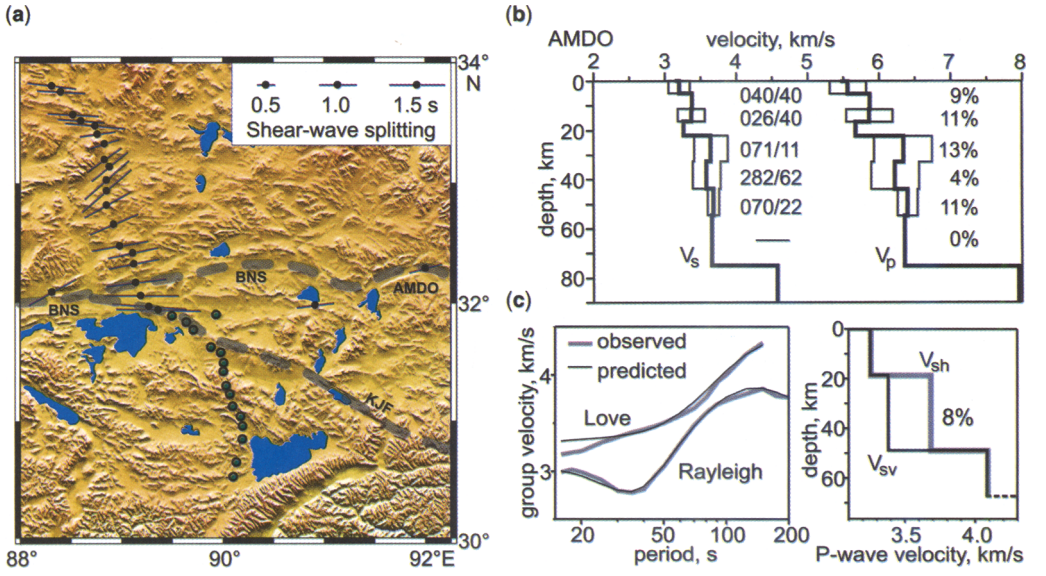

Fig. 5. Evidence for crustal seismic anisotropy. (**a**) Averaged fast directions and delay times based on SKS measurements, from Huang *et al.* (2000). Result at AMDO from McNamara *et al.* (1994). BNS, Banggong–Nujiang suture; KJF, Karakoram–Jiali fault system. Very rapid change in splitting over <10 km distance requires the anisotropy to be at least partially in the crust. (**b**) Anisotropic crustal velocity model at AMDO from receiver-function inversions, from Sherrington *et al.* (2004): vertical lines show minimum, average and maximum velocities for anisotropic layers. Numbers beside each layer are trend/plunge of fast direction and percentage anisotropy for each of five anisotropic layers. (**c**) Radial anisotropy in the Tibetan crust from Shapiro *et al.* (2004), showing on the left the surface-wave dispersion inversion for a point in western Tibet (34°N, 84°E), and the fit to the observed dispersion curves using the 8% radial anisotropy in the middle crust shown on the right. Depth scale is identical in (b) and (c).

known only from within the graben, perhaps merely because seismic-reflection coverage outside the graben is as yet sparse (Haines *et al.* 2003; Ross *et al.* 2004): seismic surface-wave studies indicate that similar low-velocity zones exist both within and beyond the graben (discussed above: Yuan *et al.* 1997).

The lack of correlation of the inferred region of partial melt with the young north–south grabens (which may be relatively superficial features, confined to the hanging wall of the STD: Cogan *et al.* 1998; Hurtado *et al.* 2001) is further demonstrated by the essential similarity of four widely spaced MT transects along the Himalayan arc (himprobe, nf/in-800, in-100, in-700: Unsworth *et al.* 2005). This similarity strongly suggests that the remarkable conductivity of southern Tibet first recognized by Pham *et al.* (1986) may be extrapolated laterally over 1000 km, counter-claims (Harrison 2006) notwithstanding. In all four transects, high mid-crustal conductivities clearly extend south of the Indus–Yarlung suture into the Tethyan Himalaya, to the North Himalayan gneiss domes (including Kangmar dome in the east, Tso Morari complex in the west: Fig. 1). The top of the conductivity anomaly appears to shallow to the south, and in the best-resolved eastern transects the anomalous region also thins to the south. This clear geometric pattern is explicitly interpreted by Unsworth *et al.* (2005) as the signature of a southward-directed channel flow; they show that reasonable assumptions about the degree of partial melt required to produce the observed conductivity result in strength reduction by a factor of about four.

Whereas the highest conductivities in southern Tibet are most reasonably explained by brines in conjunction with magma, in northern Tibet it has previously been suggested that brines do not play a significant role (Wei *et al.* 2001; Unsworth *et al.* 2004). The xenoliths that are our best record of the lower crust in the Qiangtang terrane had anhydrous mineral assemblages resistant to widespread crustal melting at the time of eruption, 3 million years ago (Hacker *et al.* 2000). Thus either brines or melts in the lower crust are likely to be derived from below, and any saline fluids have probably infiltrated the crust since 3 Ma. Irrespective of the availability of brine or melt, fluids must form a physically interconnected network to be conductive, requiring a fluid–mineral dihedral angle <60° for

typically low lithospheric fluid contents. Despite previous statements that aqueous fluids will not connect to form conductive pathways at the depths of the northern Tibet conductors (Wei *et al.* 2001), the unusual thickness of Tibetan crust ($\geq$60 km) means that the pressure dependence of dihedral angle must be considered. Though water forms dihedral angles $>60^\circ$ with typical crustal and mantle minerals in the lower crust and uppermost mantle of normal lithospheres (crust *c.* 40 km thick), at pressure (p) >1 GPa and temperature (T) $>800^\circ$C the dihedral angle is $<60^\circ$ for water in plagioclase (Yoshino *et al.* 2002) and quartz (Holness 1993) aggregates, and for water in olivine at p >1.5 GPa and T $>1000^\circ$C (Mibe *et al.* 1999). These are pT conditions presumably relevant to northern Tibet. Melts are also likely to form interconnected conductive pathways in the upper mantle, as dihedral angles for melt with olivine are low (Waff & Bulau 1979). The situation is less clear in the lower crust, as measured melt–pyroxene dihedral angles (Toramaru & Fujii 1986) and water–pyroxene dihedral angles (Watson & Lupulescu 1993) are $>60^\circ$. Thus the high observed conductivities imply fluids are present throughout the lower crust/uppermost mantle of northern Tibet, but do not necessarily require partial melt.

Seismic anisotropy: evidence for past or present strain of mantle and crust

In contrast to low seismic velocities and high electrical conductivities that show modern crustal weakness without demonstrating active deformation, the presence of seismic anisotropy requires flow (or possibly only recrystallization while under a non-uniform stress system) but cannot demonstrate that the flow is ongoing as opposed to a fossil record. In Tibet, anisotropy models have been presented at three scales: (1) plateau-wide observations of crustal anisotropy from surface waves (Shapiro *et al.* 2004); (2) regional variations in single-layer estimates of splitting of SKS (and related phases) often largely attributed to mantle deformation (e.g. SF-1, -3: Hirn *et al.* 1995; PASSCAL: McNamara *et al.* 1994; IN-3: Huang *et al.* 2000); and (3) multilayer anisotropic receiver-function inversions beneath individual stations for detailed crustal anisotropy (SF-4: Vergne *et al.* 2003; IN-3: Ozacar & Zandt 2004; PASSCAL: Sherrington *et al.* 2004).

The most ubiquitous measurements of anisotropy are those of split SKS and related teleseismic phases recorded at individual stations, most routinely presented in terms of a single delay time and orientation (e.g. Silver 1996). Such anisotropy is frequently interpreted as arising in the lithospheric mantle, because abundant olivine in the mantle allows easy creation of strain-induced lattice preferred orientation, hence significant velocity anisotropy. Most interpretations assume a single anisotropic layer, and cannot resolve delay times $\leq$0.5 s due to the long dominant periods ($>$5 s) of SKS waves. In Tibet most stations in the Tethyan Himalaya and the southern Lhasa terrane (PASSCAL: McNamara *et al.* 1994; SF-3: Hirn *et al.* 1995; IN-2: Sandvol *et al.* 1997) show modest or negligible splitting (0–1 s), representing either small or complexly distributed anisotropy. A similar lack of splitting (transverse isotropy) at stations on the Indian craton has been used to bolster the argument that subducting Indian lithosphere underlies southern Tibet (Chen & Özalaybey 1998). In contrast, stations in the Qiangtang and Songpan–Ganzi terranes show large split times (1–2 s), with orientations typically 090 $\pm$ 30° (PASSCAL: McNamara *et al.* 1994; SF-4: Herquel *et al.* 1995; IN-3: Huang *et al.* 2000). This splitting pattern beneath northern Tibet has been interpreted as representing either asthenospheric flow enabling eastward extrusion of rigid blocks of Tibetan lithosphere (Lavé *et al.* 1996) or finite strain in Tibetan lithospheric mantle (Davis *et al.* 1997) deforming by north–south shortening or east–west extension. Hirn *et al.* (1995; profile SF-3) argued that the same splitting orientation was present throughout the Lhasa terrane, albeit with smaller split times.

A remarkable observation from the densely instrumented INDEPTH-3 transect is that the transition from negligible to significant splitting occurs over a distance of only 15 km across the Jiali fault, 40 km south of the Banggong–Nujiang suture, requiring that crustal anisotropy is at least locally substantial and distinct between the adjacent stations (IN-3: Huang *et al.* 2000) (Fig. 5a). Where observed splitting parameters are more spatially coherent, further north and south along the INDEPTH-3 transect, it is harder to demonstrate the depth of anisotropy, but arguments based on seismic resolution (the Fresnel zone), suggest the anisotropy largely resides in the lower crust and upper mantle (Huang *et al.* 2000). The crustal component of Tibetan anisotropy has been further elucidated by anisotropic receiver-function analysis that suggests dipping and horizontal Vp and Vs anisotropy in multiple layers 2–25 km thick, that may be coherent across a few tens of kilometres (Ozacar & Zandt 2004) but are far harder to correlate across inter-station distances $>$100 km (Sherrington *et al.* 2004). Although individual interpretations are non-unique (significantly different structures were interpreted beneath the same station by Frederiksen *et al.* (2003), Vergne *et al.* (2003), and Sherrington *et al.* (2004)), it seems

clear that there is considerable and complex anisotropy in the crust. In part these complex anisotropies must represent a time-integrated strain history: anisotropic layers in the brittle upper crust cannot be ductilely deforming at present, so their anisotropy may represent either open cracks or old metamorphic fabrics, whereas complex patterns of mid- and lower-crustal anisotropy may represent active deformation superimposed on older strain fabrics (PASSCAL: Sherrington *et al.* 2004) (Fig. 5b). The clearest relationship yet seen between active deformation and anisotropy is the observation of a layer with 20% anisotropy aligned in the direction of plate motion at the décollement between subducting India and the Lesser Himalaya (HIMNT: Schulte-Pelkum *et al.* 2005), and this study shows the clear potential for very dense passive seismometer arrays to detect anisotropic flow channels elsewhere in Tibet, though caution is always required to discriminate the effects of dipping layers from those of anisotropy.

The large-scale behaviour of the crust may be better captured by plateau-wide inversions of surface wave anisotropy. Shapiro *et al.* (2004) averaged surface waves propagating through Tibetan crust on a 1° grid and showed that seismic velocity in the vertical direction (Rayleigh mode) is slower than in the horizontal direction (Love mode) (note this study did not resolve azimuthal variations in the horizontal wave-speed) (Fig. 5c). This observation is most simply interpreted as due to near-horizontal reorientation of anisotropic minerals – principally micas – during thinning of the anisotropic layer, because pure-shear thickening tends to produce the opposite sense anisotropy to that observed. Depending on the assumed thickness of the anisotropic layer, a vertical flattening strain of 20% (if the entire middle and lower crust below 20 km depth is deforming) to 40% (if only a 25-km-thick middle crust deforms) is required to produce the observed radial anisotropy in a rock containing 30% mica (Shapiro *et al.* 2004). (Note that such thinning may be less than the flux of Indian crust into/beneath Tibet, so may not imply net crustal thinning; cf. Kapp & Guynn 2004.) Few rocks contain as much as 30% mica, and less micaceous rocks would require larger strains to develop the same anisotropy. Although this observed anisotropy could in principle represent effects of deformation before the Himalayan collision and/or younger events, it is clearly present beneath both the Lhasa and Qiangtang terranes, and arguably also beneath the Tethyan Himalaya and Songpan–Ganzi terrane (Shapiro *et al.* 2004). As with the reflective layering of the lower crust observed both north and south of the Banggong–Nujiang suture (discussed below) (IN-3: Ross *et al.* 2004), the simplest interpretation is that both the radial anisotropy and the crustal reflectivity represent an ongoing flattening flow in a 25–50 km thick mid-to-lower crust.

Seismic reflectivity: evidence for fluids and flow

INDEPTH has recorded *c.* 350 km of multifold seismic reflection data (Fig. 1) that were used to interpret the structural development of the Himalayan thrust belt (IN-1: Zhao *et al.* 1993; IN-2: Hauck *et al.* 1998), the Indus–Yarlung suture zone (IN-2: Makovsky *et al.* 1999) and the southern Lhasa terrane (IN-2: Alsdorf *et al.* 1998*a*). Observations particularly germane to crustal rheology are unusually high-amplitude reflections ('bright spots') that may represent magmatic (Brown *et al.* 1996) or aqueous (Makovsky & Klemperer 1999) fluids, and analyses of crustal reflectivity (Ross *et al.* 2004) (Fig. 6).

The bright-spot observations on the INDEPTH-2 profiles, restricted by lack of data elsewhere to the Yangbajain graben and geothermal province of the southern Lhasa terrane, are: (1) unusually strong amplitudes recorded from a depth of *c.* 15 km below the surface, which require unusual lithologies or fluids, possibly in layers thinner than the seismic wavelength (*c.* 10^2 m) that act to enhance the amplitudes (Brown *et al.* 1996) (Fig. 6a); (2) strong P-to-S-wave seismic conversions at these reflectors, which require the presence of fluids (Makovsky & Klemperer 1999); (3) a variation of amplitude with incidence angle of these reflections that seems to indicate a fluid that is dominantly aqueous in >15% porosity (Makovsky & Klemperer 1999), though this last measurement is one with large uncertainties. Incontrovertibly, the crust below the Yangbajain graben contains magma and/or free aqueous fluids. If magma is present, the temperature must exceed the minimum granitic melt temperature at 15 km depth (*c.* 650°C: e.g. Thompson & Connolly 1995) given the large percentage volume of melt indicated, unless we have fortuitously imaged very recent intrusions prior to their cooling and freezing. If instead the crust contains aqueous fluid, it does so in volumes too large to be easily maintained over geological time periods without replenishment (Bailey 1990; Warner 1990), thereby implying a fluid source at depth, possibly subducting India. Even small percentages of free water in the crust are likely to trigger partial melting at temperatures above the minimum melt of granite. Whether water or melt is present, the crust is likely to be weakened. These bright spots were interpreted by Nelson *et al.* (1996) and Wu *et al.* (1998) as melts of Indian and Asian crust that will in the future be exposed at the surface in a return channel flow as

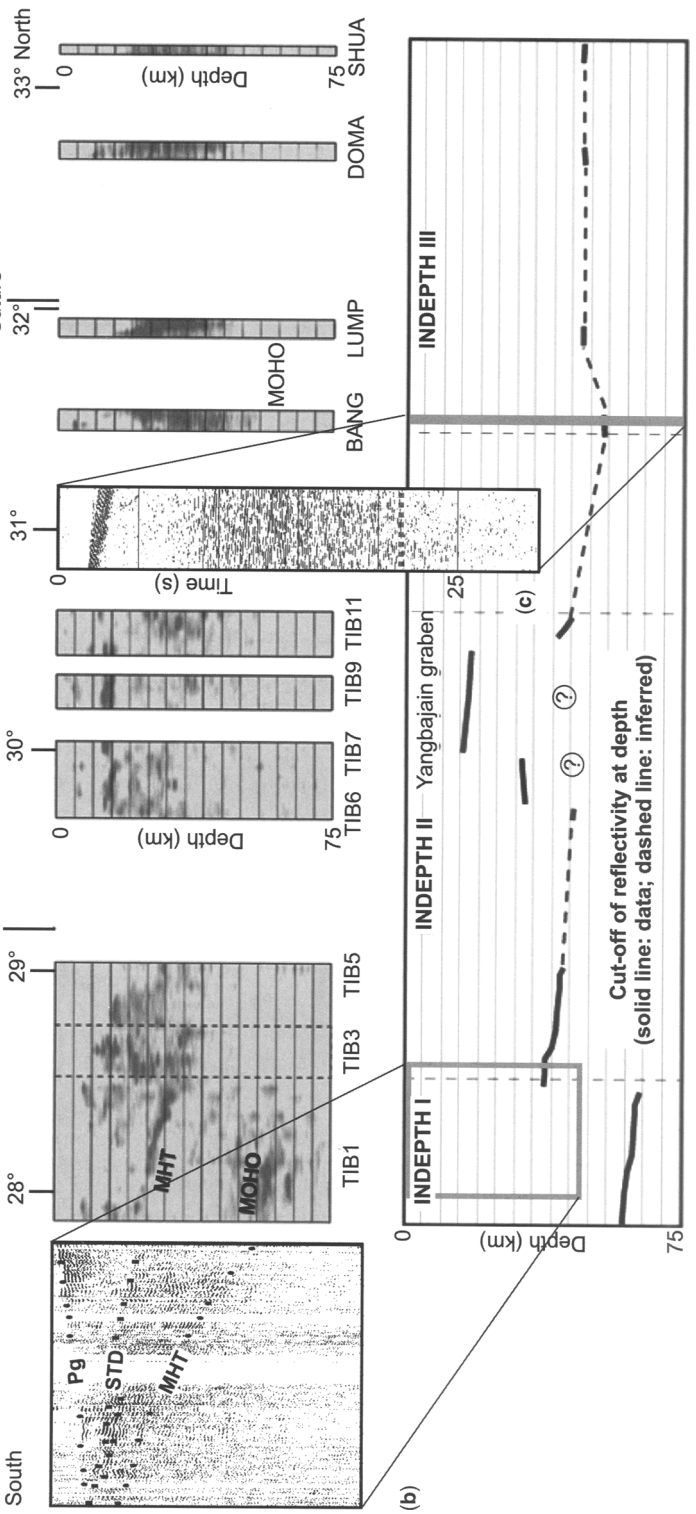

Fig. 6. Vertical distribution of crustal reflectivity from INDEPTH profiling along *c.* 90°E. (**a**) Reflection strength along INDEPTH stacked vertical reflection profiles (above) and interpreted cut-off of reflectivity at depth (below). From the south: on profile TIB-1 (IN-1), clear Moho and Main Himalayan Thrust (MHT) reflections are seen; on TIB-1, -3 and -5 (IN-2) reflectivity is strongest above the MHT; TIB-6, -7, -9 and -11 (IN-2) are dominated by reflectivity around 15 km depth (seismic bright spots) but question marks indicate uncertainty as to whether high attenuation is preventing observation of reflective layering at depth; from the middle of TIB-11 north, including profiles BANG, LUMP, DOMA and SHUA (IN-3), mid-crustal reflectivity is replaced by lower-crustal reflectivity that terminates at the Moho. Vertical exaggeration is ×2. After Ross *et al.* (2004). (**b**) Inset of wide-angle reflection data (time-domain receiver gather with reduction velocity of 6 km s^{-1}) at south end of profile; approximate extent shown by grey box on reflectivity cut-off plot, showing prominent reflectivity between STD and MHT. Pg is direct wave. Note that upward convergence of STD and MHT to the south is an artifact of the receiver-gather display in which true geometries are highly distorted; these reflectors are actually subparallel. After Makovsky *et al.* (1996). (**c**) Inset of near-vertical reflection data (time-domain shot gather with no move-out) from BANG profile, at same vertical (travel-time) scale as inset (b) but very different horizontal (distance) scale, to show absence of upper-crustal reflectivity and clear middle-to-lower-crustal reflectivity; amplitude–decay curves show shot energy extends below Moho (interpreted at 22 s travel-time (63 km), grey dotted line) so reflectivity cut-off has tectonic significance. After Ross *et al.* (2004).

High Himalayan leucogranites. This interpretation of leucogranitic melt is permitted but not required by the seismic and MT observations. If a return channel flow exists bounded below by the MHT and above by the STD, then crystallized analogues of the bright spots may be expected to be present in the subsurface beneath the Tethyan Himalaya. It has been suggested that bright reflections with a characteristic upward concavity above the MHT (Alsdorf *et al.* 1998*b*) may represent such intrusions (L. D. Brown, pers. comm. 2004) analogous to saucer-shaped sills now routinely mapped on 3D seismic reflection data over volcanic rifted margins (e.g. Thomson 2004). However, modelling suggests that these saucer shapes develop only at shallow depths, when their length exceeds the depth by a factor of two to three (requiring 30–45 km long sills for the intrusion depth of 15 km suggested by INDEPTH data) (Malthe-Sørenssen *et al.* 2004); and the apparent curvature on INDEPTH profiles may be an artifact of 2D seismic migration of the INDEPTH data.

Pronounced 'lower-crustal' reflectivity seen elsewhere on Earth is commonly thought to result from tectonically imposed layering, including shear zones (e.g. Green *et al.* 1990) and/or multiple horizontal planar mafic intrusions ('sills') (e.g. Warner 1990). The characteristic reflectivity is bounded below by the Moho, and in many tectonically active locations dies out upwards at about the brittle–ductile transition (e.g. Klemperer 1987; Holbrook *et al.* 1991). Ross *et al.* (2004) show that in the northern Lhasa and southern Qiangtang terranes (IN-3, Fig. 1), strongly reflective crust exists from 25 km to the Moho at *c.* 65 km depth (Fig. 6a & c). Beneath the Yangbajain graben no lower-crustal reflectivity is observed (except on the northernmost profile); however, amplitude analysis of these data shows that reflected energy is a factor of three to ten below comparable values for INDEPTH-III, consistent with a hypothesis that the observed high reflectivity of the bright spots, and observed high attenuation of the upper crust (Xie *et al.* 2004) due to hydrothermal activity there, prevents observations of a lower crust that is in fact reflective (Ross *et al.* 2004). The lack of high velocities in most of the crust (IN-2: Kola-Ojo & Meissner 2001, IN-3: Zhao *et al.* 2001) is an argument against widespread mafic intrusions as an explanation of the observed reflectivity, and there is no obvious magmatic event recorded at the surface in either the Qiangtang or the Lhasa terrane to which mafic intrusions may be linked. The most plausible interpretation is that the reflective zone represents a region of active ductile deformation and flattening foliation, such as would be produced in a region undergoing extensional flow, or having undergone such flow as the most recent tectonothermal event (Ross *et al.* 2004). This reflective zone demonstrably occupies the entire middle and lower crust in the Qiangtang and northern Lhasa terranes in the few locations where profiling has been undertaken; it may occupy the entire middle and lower crust in the southern Lhasa terrane, though obscured by shallow attenuating bodies; and it is demonstrably limited to the upper crust in the Tethyan Himalaya (Ross *et al.* 2004). Reflectivity is particularly pronounced below the STD and above the MHT, even south of the North Himalayan gneiss domes (Fig. 6b) (IN-1: Makovsky *et al.* 1996), hence south of MT or geothermal evidence for young intrusive activity. Cooled felsic intrusions would not produce substantial reflectivity within the GHS, and the moderate seismic velocity within the reflective zone $<6.2\ \mathrm{km\ s^{-1}}$ (Makovsky *et al.* 1996) precludes a large number of mafic intrusions, so the reflectivity seems most likely to represent older flow-related flattening structures.

Some indirect temperature estimates

Direct measurements of crustal heat flow and inference of high lower-crustal temperature are corroborated by a variety of less direct approaches. Alsdorf & Nelson (1999) model the pronounced satellite magnetic low observed over Tibet as indicating that the Curie isotherm (*c.* 550°C) resides in the upper crust (*c.* 15 km depth) across the entire plateau. Mechie *et al.* (2004) believe they can identify the $\alpha - \beta$ quartz transition as a seismic reflector along the INDEPTH-3 transect, thereby constraining the temperature to be 700°C at 18 km depth in the southern Qiangtang terrane, and 800°C at 32 km depth in the northern Lhasa terrane. Hacker *et al.* (2000) describe xenoliths from the Qiangtang terrane that equilibrated at $\geq$800–900°C at depths of 30–50 km before reacting with magma at 1300°C in the lower crust and entrainment in a 3 Ma eruption. Initial estimates of uppermost mantle temperature from Pn tomography were 840–1170°C, lower beneath the Lhasa terrane, higher beneath the Qiangtang (McNamara *et al.* 1997). However, the lateral temperature difference is much better determined than the absolute temperatures. Uncertainties in experimental elastic and anelastic parameters and in seismic velocities do not allow absolute constraints from seismic velocities any tighter than $\pm$150°C (Goes & van der Lee 2002), and the Pn velocities are also consistent with temperatures in the seismogenic upper mantle beneath the Lhasa terrane of <750°C, and upper mantle beneath the northern plateau in the range 950–1100°C (Ruppel & McNamara 1997). Although the abundant Late Miocene to Recent potassic volcanics of northern Tibet have been interpreted as representing high temperature

(*c.* 1100°C) melting of the subcontinental mantle, this temperature was probably not attained above *c.* 125 km depth, well below the Moho (Turner *et al.* 1996). Miocene (but none yet younger than 8 Ma) potassic volcanics are also known from southern Tibet (Ding *et al.* 2003), representing lower degrees of partial melt (Williams *et al.* 2004), therefore presumably lower melting temperatures than in northern Tibet, and are coupled with calc-alkaline adakites of the same age range that may represent partial melts of an eclogitic lower crust (Chung *et al.* 2003). The youngest igneous rocks in southern Tibet (away from the syntaxes) are *c.* 7 Ma leucogranites (Li *et al.* 1998) and though these only indicate relatively shallow (600–800 MPa), relatively low-temperature (750–800°C) melting (Patino Douce & Harris 1998), the time for conductive cooling of material at *c.* 20 km depth is >10 Ma (e.g. Lachenbruch & Sass 1977) so that the south Tibetan mid-crust cannot be substantially cooler now than it was during melt formation at 7 Ma.

Finally one may mention temperature estimates based on two-dimensional finite-element methods, that seek to model effects of the geometry of India underthrusting from the south and frictional heating on faults; convergence rates and erosion rates at the southern margin of Tibet; radiogenic heat production in the crust, and mantle heat flow, etc., either in steady-state kinematic models (Henry *et al.* 1997; Huerta *et al.* 1998) or in coupled thermal–mechanical models (Beaumont *et al.* 2004; Jamieson *et al.* 2004). These models are of most value in southern Tibet where constrained by geometries indicated by the INDEPTH and other seismic transects. The Henry *et al.* (1997) model predicts crustal temperatures south of the Indus–Yarlung suture, where they suggest that temperatures of 550–850°C may be attained in the core of the orogenic wedge, just above the MHT at *c.* 40 km depth, with lower temperatures of 500–600°C at the base of the crust at *c.* 80 km depth. Approximately doubling the mantle heat flow can increase these temperatures to 950°C and 750°C, respectively. An extension of this model into the Lhasa terrane (Cattin *et al.* 2001) gives Moho temperatures of *c.* 550–700°C. Beaumont *et al.* (2004) predict higher maximum crustal temperatures of 900°C and 800°C at the same locations, and suggest that Moho temperatures increase to about 900°C in the Lhasa terrane and 1000°C beneath the Qiangtang. Although predicted temperatures vary considerably with assumptions about poorly constrained parameters (e.g. radiogenic heat production and mantle heat flow), sensible parameter choices yield temperatures consistent with the geological and geophysical observations above.

Physical properties inferred from geophysical observations

Inferred vertical strength profiles

In southern Tibet, the observation of sub-Moho earthquakes (Chen & Yang 2004; Monsalve *et al.* 2006) implies the crust is weaker than deeper layers. Even if the earthquakes at 80–90 km are above the Moho (Jackson 2003; Mitra *et al.* 2005) or in eclogitized crust now below the Moho as possibly recognized seismically (Sapin & Hirn 1997) or by the adakitic products of their melting (Chung *et al.* 2003), the relative absence of seismicity from *c.* 20 to 70 km demonstrates a broad channel in which deformation is accommodated by ductile, not brittle processes (Fig. 7a). This crust has lower-than-normal P-wave velocities (Hirn *et al.* 1984*a*; Owens & Zandt 1997; Rodgers & Schwartz 1998; Haines *et al.* 2003), lower-than-normal S-wave velocities (Cotte *et al.* 1999; Rapine *et al.* 2003), an intra-crustal S-wave low-velocity zone (Kind *et al.* 1996), and seismic reflectivity (Makovsky & Klemperer 1999) and electromagnetic conductivity (Li *et al.* 2003) indicative of fluids, all suggesting that the crust is unusually weak. This weakness is consistent also with the high conductive heat flow (Shanker *et al.* 1976; Francheteau *et al.* 1984), vigorous geothermal activity (Hochstein & Regenauer-Lieb 1998) and short-wavelength flexural topography (Masek *et al.* 1994) of southern Tibet. Evidence that magmatic intrusion (Gupta *et al.* 1983; Jaupart *et al.* 1985) and maximum concentrations of fluids (Unsworth *et al.* 2005) are in the upper crust, and that the intra-crustal low-velocity zone may not extend to the lower crust (Kind *et al.* 1996; but see also Cotte *et al.* 1999) suggest that the low-strength channel may be localized in the middle crust and may not include the lower-crust (Figs 3 & 7a).

This region with a strength minimum in the middle crust includes the Tethyan Himalaya at least as far south as the North Himalayan gneiss domes, based on the conductivity anomalies (Unsworth *et al.* 2005) and measurements of high heat flow (Gupta *et al.* 1983; Francheteau *et al.* 1984). A dramatically weaker mid-crust does not extend significantly further south based on the disappearance of the highest conductivities and heat flow, the rapid decrease in seismic attenuation (Xie *et al.* 2004), and the southward decrease in crustal temperatures required by any reasonable thermal model (Henry *et al.* 1997; Huerta *et al.* 1998). The crustal weak zone presumably includes much of the Lhasa terrane, extending to the northern edge of colder south-Tibetan mantle that is crudely placed beneath the Banggong–Nujiang suture by Pn and Sn velocity tomography

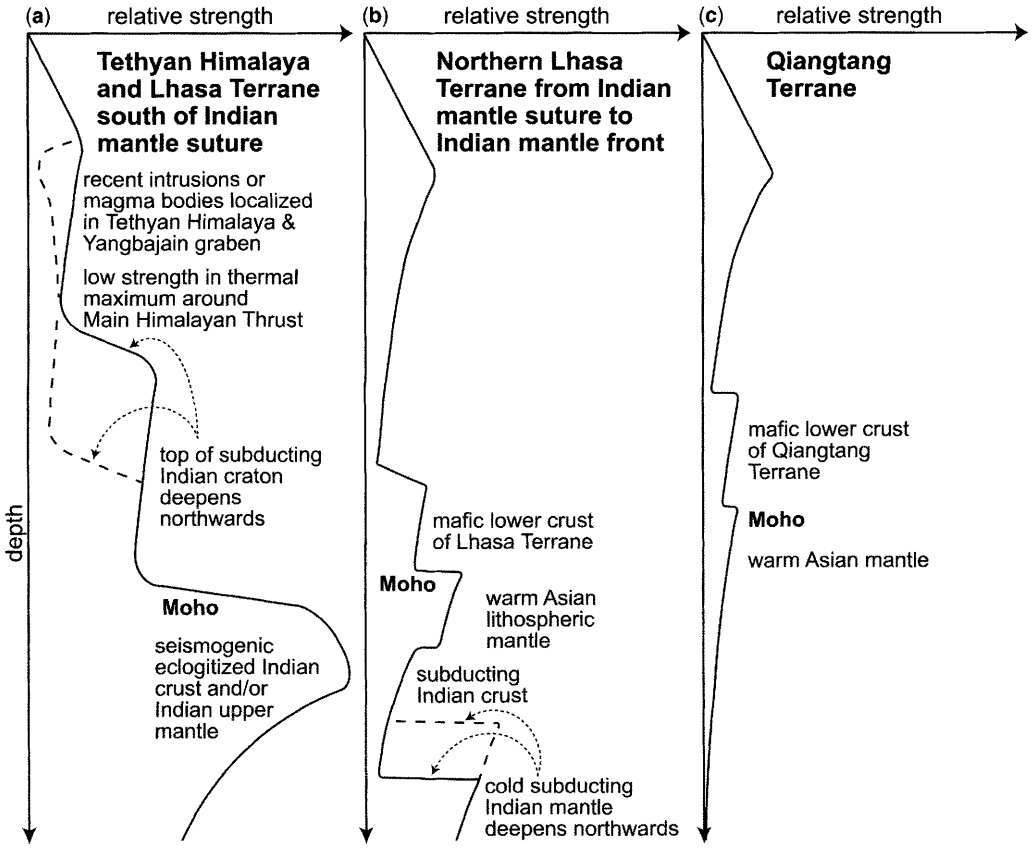

Fig. 7. Cartoons of inferred relative strength–depth profiles for Tibet at about 90°E. The competing effects of increasing temperature with depth and compositional variability (generally more mafic at depth) allow multiple weak channels in the lithosphere. (**a**) In the Tethyan Himalaya and southern Lhasa terrane the greatest lithospheric strength is likely in the seismogenic upper mantle. Dashed lines represent laterally variable conditions. (**b**) In the northern Lhasa terrane north of the Indian mantle suture it is uncertain whether the upper crust or upper mantle is stronger, but the weakest zone is probably at the base of the middle crust. (**c**) In the central and eastern Qiangtang terrane the only significant lithospheric strength is probably in the brittle upper crust; west of *c.* 85°E the mantle may become somewhat colder and stronger.

(McNamara *et al.* 1995, 1997; Tilmann *et al.* 2003). A better resolved measure of the change in mantle properties may be the clear change in mantle anisotropy at the Jiali fault system (Huang *et al.* 2000), which has recently been suggested to reach through the crust to the Moho based on receiver-function imaging (Galvé *et al.* 2002*b*) and crustal refraction data (Zhang & Klemperer 2005). A plausible suggestion is that this boundary represents the northern limit of Indian cratonic mantle in contact with the Moho (Beghoul *et al.* 1993; Jin *et al.* 1996; Tilmann *et al.* 2003), either the leading edge of Indian lithosphere, or its northernmost extent before it bends sharply down to the north. It is possible that a thin zone of warmer Asian mantle still overlies the Indian lithosphere (from *c.* 30°N, the 'mantle suture' of Jin *et al.* (1996) to *c.* 32°N, their 'mantle front'), as indicated by mantle-derived helium emissions in this region (Hoke *et al.* 2000). The presence of a thin zone of warm Asian mantle above cold Indian mantle would not remove the strength minimum, though could potentially lead to a more complex strength profile in which uppermost (Asian) mantle forms part of the weak zone (Fig. 7b).

In northern Tibet the situation is less clear-cut. There is overwhelming evidence that the crust is unusually weak by global standards because it is thick (Owens & Zandt 1997; Vergne *et al.* 2002), low-velocity (Rodgers & Schwartz 1998; Rapine *et al.* 2003), seismically attenuating (Rodgers & Schwartz 1998; Fan & Lay 2003), hot

(Hacker *et al.* 2000; Mechie *et al.* 2004), and contains a few per cent of fluids (Unsworth *et al.* 2004). However, the upper mantle of northern Tibet is also low-velocity after appropriate temperature correction (Rodgers & Schwartz 1998), is also seismically attenuating (Ni & Barazangi 1983; McNamara *et al.* 1995), and probably also contains fluids (Unsworth *et al.* 2004) at least east of *c.* 85°E (Barazangi & Ni 1982; Dricker & Roecker 2002) (at present we lack detailed observations of the Qiangtang mantle from broadband seismic deployments at 82–88°E: Fig. 1). Some have argued for removal of the entire lithospheric mantle of northern Tibet and its replacement by asthenospheric material (Molnar *et al.* 1993; Willett & Beaumont 1994), perhaps due to subduction of Indian and Asian lithospheres (Kosarev *et al.* 1999; Kind *et al.* 2002; Shi *et al.* 2004) which would limit the region of upwelled asthenosphere to south and north respectively. However, recent estimates of depth to the lithosphere–asthenosphere boundary strongly suggest that >100 km lithospheric mantle is present everywhere beneath Tibet (Priestley & McKenzie 2006), albeit somewhat thinner beneath the Qiangtang than beneath the Lhasa terrane (Kumar *et al.* 2006).

The clear anisotropy observed in both crust (Shapiro *et al.* 2004; Sherrington *et al.* 2004) and mantle (McNamara *et al.* 1994; Huang *et al.* 2000) suggests both layers are deforming at the present by distributed strain. It is therefore not certain whether the mantle is weaker than the crust, or vice versa (Fig. 7c). The clear lower-crustal and Moho conversions on receiver functions across northern Tibet (Owens & Zandt 1997; Vergne *et al.* 2002) demonstrate a significant impedance increase at the top of the mafic lower crust and mantle, requiring rapid changes in lithology. If temperatures are in conductive equilibrium at the Moho, and fluids are present both above and below the Moho (Unsworth *et al.* 2004), then it seems most likely that there are increases in strength with depth at the top of a mafic lower crust and at the Moho, irrespective of whether the middle-lower crust or upper mantle possesses the larger total strength (Fig. 7c).

Inferred vertical velocity profiles

In southern Tibet, the surface is moving approximately NNE with respect to stable Eurasia (Wang *et al.* 2001; Chen *et al.* 2004). The lower lithosphere must have the same sense of motion, because the Indian plate is underthrusting Tibet at the Himalayan front, and converging with Eurasia in the same direction at the same or higher speed as GPS stations located in and north of the Tethyan Himalaya (Wang *et al.* 2001). Similar focal mechanisms in the south Tibetan upper crust and upper mantle (Molnar & Chen 1983) are consistent with identical kinematics at these different depths, whether or not they are decoupled by the relatively aseismic middle and lower crust. However, erosion is continuously removing significant amounts of material from the Himalaya (Johnson 1994; Galy & France-Lanord 2001), in a discontinuous manner highly focused at the topographic front (Wobus *et al.* 2003). Presuming the mountain front is not rapidly migrating northwards due to erosional retreat (Avouac 2003), the eroded material must be continuously replenished by some form of deformation, whether channel flow (Grujic *et al.* 2002; Searle & Szulc 2005) or thrust wedging (Grasemann & Vannay 1999), thereby advecting material southwards from Tibet to the Himalayan front (Hodges *et al.* 2001; Beaumont *et al.* 2004). Hence for at least southernmost Tibet there should be a reduced northward velocity (with respect to stable Eurasia) in the middle crust with respect to the upper crust and the upper mantle (Fig. 8). This is by definition a channel flow. The flow may be largely of Poiseuille form, driven outwards from the plateau by gravitational potential energy, but presumably also experiences a northward basal drag due to underthrusting of India (a Couette-type component – Fig. 2b) (Beaumont *et al.* 2004). It is at least plausible that this southward-directed flow (with respect to superjacent and subjacent layers) extends with diminishing vigour as far north as the inferred Indian mantle front at about the position of the Jiali fault.

North of the Jiali fault, the eastward velocity of Tibetan crust from GPS measurements reaches as much as 50% of the total convergence between India and Asia in the eastern part of the plateau (Chen *et al.* 2004; Zhang *et al.* 2004) (no data are available for the western Qiangtang). The continuity of the strain field over hundreds of kilometres as measured on tens of stations in single transects shows that this eastward motion is not that of a relatively undeforming block bounded by rapidly moving strike-slip faults, as suggested by past extrusion models (Tapponnier *et al.* 1982, 2001), but instead is driven by more-distributed east–west extension in response to the north–south convergence across Tibet. Clearly northern Tibet is deforming in an essentially continuous manner, and the lower crust and upper mantle must both be deforming by flow because they are weak (Fig. 8). Strong anisotropy in both the crust (Shapiro *et al.* 2004) and mantle (McNamara *et al.* 1994; Huang *et al.* 2000) reflect this modern strain field. The correlation of the surface strain field (from GPS) with the mantle strain field (from SKS splitting) could simply result if the crust and mantle lithosphere are under similar boundary conditions (Holt 2000);

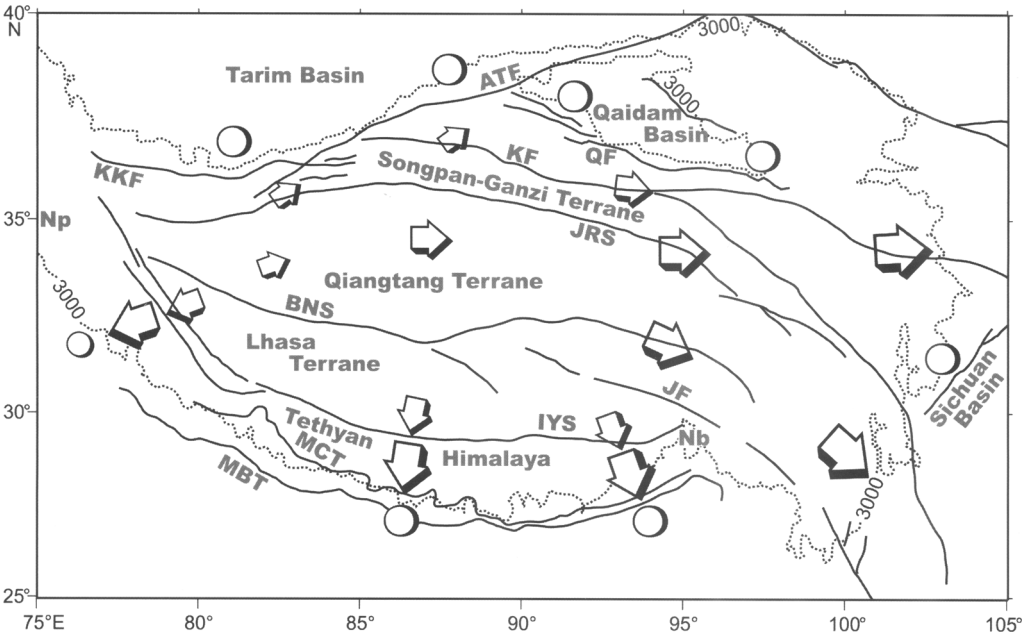

Fig. 8. Suggested directions of middle/lower-crustal channel flow in Tibet (open arrows) and regions of no flow (open circles). Gravitational potential energy and orographic exhumation drive a south-directed Poiseuille-type flow between subducting Indian lower lithosphere and brittle upper crust of Tethyan Himalaya and southern Lhasa terrane. Southern boundary of this flow province is the Himalayan topographic front; northern boundary may be the Jiali fault in the east, and the Karakoram–Jiali system or Banggong–Nujiang suture in the west. North–south compression and east–west extension of northern Tibet drives a mixed Poiseuille/Couette-type flow eastwards beneath the Qiangtang terrane, which bifurcates north and south of the rigid Sichuan basin. Northern boundary of this flow province is the Karakax–Altyn Tagh fault system bounding the rigid Tarim basin, and the Qaidam border fault south of the Qaidam basin, which both mark large and abrupt changes in crustal thickness. Arrows cross-cutting faults/sutures represent interpreted flow at depth beneath upper-crustal faults, including Kunlun fault, Jinsha River suture, and Banggong–Nujiang suture. See caption to Figure 1 for abbreviations.

all levels in the lithosphere may be flowing in the same direction, but with different velocities and strain rates. Tikoff *et al.* (2004) have argued that global evidence for compatible upper-crustal and upper-mantle deformation implies at least partial mechanical coupling between these layers; they suggest that bottom-driven systems must be the general rule in orogens since tectonic movements ultimately result from deep-mantle processes. If applied to northern Tibet this argument would seem to ignore the profound weakness of the lower lithosphere that can hardly drive deformation in the strong upper crust. Flesch *et al.* (2005) provide a stronger argument for crust–mantle coupling in Tibet: they use dynamic modelling of Eurasian deformation to show that plate-tectonic boundary conditions and topographically induced body forces are roughly equal; but because the body forces are applied to the crust, they can only contribute to mantle deformation if crust–mantle coupling is strong. Flesch *et al.* (2005) go on to argue that the vertically coherent deformation implied by equivalence of GPS- and SKS-derived strain fields implies that mantle deformation in Tibet is driven by upper-crustal dynamics through a strong crust–mantle coupling that is 'incompatible with the "jelly-sandwich" rheology' and 'precludes large-scale lower crustal flow or mantle delamination' as described by Willett & Beaumont (1994), Clark & Royden (2000) and Beaumont *et al.* (2004). This seems too strong a conclusion and ignores the likelihood that the middle crust is the weakest part of the lithosphere throughout much of Tibet (Fig. 7b & c). Comparison of Rayleigh and Love wave velocities implies a strong flattening anisotropy throughout Tibet that has apparently thinned the middle crust more than the upper crust (Shapiro *et al.* 2004), while seismic-velocity measurements (above) suggest there is at least some strength increase from the low-velocity middle to the higher-velocity lower crust, and from the mafic lower crust to the mantle. The probable strength

increases at depth in the lithosphere, and the likelihood that the observed anisotropy represents active deformation, point to a channel flow with a Couette-type component driven by the strong upper crust, in addition to the Poiseuille flow predicted by Clark & Royden (2000). There could even be total decoupling of the upper crust and upper mantle by a very weak mid-crustal layer (Royden *et al.* 1997; Shen *et al.* 2001), with the strong upper crust deforming under the influence of both lateral boundary forces and body forces, and the stronger upper mantle deforming under the influence of lateral boundary forces and basal drag.

The northern boundary of this proposed flow regime in northern Tibet with mixed Poiseuille–Couette characteristics is presumably the Karakax–Altyn Tagh–Qaidam border fault, which marks an abrupt change into thinner crust (Zhu & Helmberger 1998; Kao *et al.* 2001; Vergne *et al.* 2002; Wittlinger *et al.* 2004) overlying a seismically faster, colder and stronger mantle (Wittlinger *et al.* 1998; Zhao *et al.* 2006). In mirror image of the Himalayan thrust front, the older, colder Tarim and Qaidam lithosphere is underthrusting southwards beneath Tibet along these faults (e.g. Kao *et al.* 2001; Kind *et al.* 2002) but the low erosion rates at the northern margin of Tibet prevent the emergence there of a channel flow similar to that at the Himalayan front (Willett 1999).

The least studied area of Tibet is the west-central Qiangtang terrane (Fig. 1). If lower-crustal material cannot escape northward across the Karakax–Altyn Tagh fault, either no channel flow is occurring here or, I speculate, flow is generally out to the east to replenish material and provide continuity of the flow interpreted beneath the eastern Qiangtang (Fig. 8). The western Qiangtang has the strongest crustal radial anisotropy of any part of Tibet in the interpretation of Shapiro *et al.* (2004), and the nearest SKS splitting measurements (that combine crustal and mantle anisotropy) at 80°E (Herquel 2005) and 88°E (Huang *et al.* 2000) are generally oriented NE to east, consistent with a uniform flow pattern across the Qiangtang terrane. The western limit of this northern Tibetan flow regime (Fig. 8) is unknown. However, high crustal attenuation consistent with at least some partial melt extending west beyond 80°E (Fan & Lay 2002) coupled with possibly higher mantle velocities beneath northwestern Tibet (Dricker & Roecker 2002; but see also McNamara *et al.* 1997) indicate a pronounced low-strength channel in the mid-lower crust at least to 80°E. Hence mid-lower crustal flow may also be active in far western Tibet where north–south narrowing of the orogen is suggestive of the need for larger magnitudes of extrusion and crustal escape than further east, and where the highest average elevations on the plateau offer additional driving forces.

Evaluation of existing channel-flow models: southern Tibet

For the Himalaya and southern Tibet the geophysical observations and the implied rheological properties suggest flow is presently occurring in the inevitable strength minimum in the mid-to-lower crust, and is likely south-directed to compensate for orographic exhumation (Fig. 8). This is presumably not the precise model of Nelson *et al.* (1996) or of Beaumont *et al.* (2004), since newer data cast doubt on some aspects of these models, encouraging their further refinement. For example Nelson *et al.* (1996) predicted that the protolith for the channel material north of the Indus–Yarlung suture would be Asian (Lhasa block) crust, because the magmas inferred from seismic bright spots at 15 km depth in the Yangbajain graben (Brown *et al.* 1996) are within Asian crust in all reasonable interpretations of INDEPTH reflection data (IN-2: Alsdorf *et al.* 1988*a*; Makovsky *et al.* 1999). However, a decade of new isotopic data makes it clear that GHS rocks exposed between the MCT and STD have Indian, not Asian affinity (e.g. Myrow *et al.* 2003; Harrison 2006). Either sufficiently northern parts of the channel are not yet returned to the surface or, ironically, the seismic bright spots that were a significant original motivation for the Nelson *et al.* (1996) model of channel flow do not participate in the exhumed channel. This need not preclude a conceptually similar channel flow at greater depth: in the Beaumont *et al.* (2004) and Jamieson *et al.* (2004) model the return channel flow is confined beneath the Indus–Yarlung suture which is modelled to extend at mid-crustal levels for >200 km north of the surface position of the suture. Even newer data show that Miocene (21–8 Ma) granitoids uplifted from 12 to 15 km depth in the Nyainqentanghla Range, immediately NW of the Yangbajain graben (Fig. 1), lack the Indian isotopic component (Kapp *et al.* 2005; Harrison 2006) that might be expected from a deeper, partially molten Indian crust; and some 11.5 Ma dykes south of the Indus–Yarlung suture zone show the same isotopic characteristics, i.e. represent Asian-affinity material south of the suture (King *et al.* 2005). Though these isotopic measurements argue against one specific formulation of the channel-flow model, they are additional evidence for crustal flow, as they require a crustal magmatic system in the Lhasa terrane throughout the Miocene (hot hence weak crust: D'Andrea *et al.* 2001; Kapp *et al.* 2005) and require southward transport of Asian material beneath the surface suture (lateral displacement with respect to upper crust: King *et al.* 2005) These new isotopic data might be satisfied by a geological history in which the Indian mantle

suture did not reach north of the Nyainqentanghla Range until after 8 Ma (after the youngest magmas intruded; D'Andrea *et al.* 2001), and by a channel-flow model incorporating spatially variable material properties (Beaumont *et al.* 2006), thereby allowing more complex flow geometries and the potential for mixing of material north and south of the Indus–Yarlung suture.

Most measurements, geological or geophysical, do not adequately discriminate between different competing models in southern Tibet. For example, shallowing thermal (Jaupart *et al.* 1985) and conductivity (Unsworth *et al.* 2005) anomalies at the latitude of the North Himalayan gneiss domes match predictions of channel flow in Beaumont *et al.* (2004), but do not require it: they could be ascribed to gneiss diapirism (Lee *et al.* 2004) triggered by an underthrust ramp or overburden extension whether or not a flow channel is present at depth. The concentration of seismic reflectivity above the Main Himalayan Thrust and below the STD (Fig. 6b; Makovsky *et al.* 1996; Ross *et al.* 2004) also matches a prediction of the Beaumont model, but could equally be explained as deformation within an extruding thrust wedge or a conventional ductile thrust duplex. Similarly, ductile shear strain and out-of-sequence thrusting that have been considered diagnostic of channel-flow models are equally compatible with conventional thrust behaviour (e.g. Robinson & Pearson 2006). However, the large-scale fold-and-thrust-belt geometry of the Himalaya, and the coherent right-side-up stratigraphic succession of the Greater and Lesser Himalayan Sequences (e.g. Harrison 2006; Robinson & Pearson 2006) seem inconsistent with the wholesale mixing during channel flow shown by current numerical realizations of channel-flow models (Beaumont *et al.* 2004; Jamieson *et al.* 2004) in which apparent stratigraphy does not always represent original relationships (Jamieson *et al.* 2006).

Most flow models are created *a posteriori* to explain existing data, and will continue to be revised to better fit newer data. Nonetheless, one can conceive measurements that might discriminate between some specific models. Continuing coeval motion of the MCT and STD is a requirement of the Nelson *et al.* (1996) and Beaumont *et al.* (2004) channel-flow models, and also of the extruding wedge concept (Burchfiel & Royden 1985), but is not required by conventional thrust belt behaviour. It is debated whether the STD and MCT are presently inactive (Searle & Szulc 2005) or are still active today (Hurtado *et al.* 2001) and hence capable of acting as boundaries of a modern channel flow, ductile at depth but exhumed at the surface by brittle processes. High-resolution seismic reflection data could track the MCT and STD to depth: the extruding wedge hypothesis suggests these two structures should meet at depth but channel-flow models predict that they do not, so that a clear image of the STD merging with the MCT at depth would refute channel flow at that location. Thus far, INDEPTH reflection data suggest a reasonable uniformity of thickness of the 'channel' between the STD and MHT for 100 km from surface outcrop of the STD to the North Himalayan gneiss domes (Kangmar Dome, Fig. 1) (IN-1: Hauck *et al.* 1998), albeit in an area of substantial along-strike structural complexity (Wu *et al.* 1998), but do not unequivocally image both the STD and MHT beneath or north of the Indus–Yarlung suture (IN-2: Alsdorf *et al.* 1998*a*; Cogan *et al.* 1998; Makovsky *et al.* 1999). Channel-flow models require pervasive deformation, hence strong seismic anisotropy, within the channel, whereas the thrust-duplex model permits passive underthrusting of relatively undeformed slices though it is also consistent with ductile flow and transposition of rocks between the STD and MCT. Thus while falsification of the hypothesis of modern channel flow in southern Tibet seems clearly possible (though certainly not yet accomplished), clear proof seems more difficult. Perhaps the closest to a demonstration that is likely to be achieved in the foreseeable future, of a channel flow following the intellectual construct if not the precise details of Nelson *et al.* (1996), would be the observation of strong anisotropy between and parallel to STD and MCT reflections that continue from outcrop north beyond the Indus–Yarlung suture.

Evaluation of existing channel-flow models: northern and eastern Tibet

For northern and eastern Tibet, the most explicit channel-flow models yet proposed are the pure Poiseuille 2D model of Clark & Royden (2000) and the 3D Newtonian viscous model of Shen *et al.* (2001) that predicts a Poiseuille-dominated flow. The Clark & Royden model is a simple 2D model that provides an excellent fit to the only data it seeks to match, the low-gradient topographic slope at the NE and SE plateau margins, but suggests unrealistically low viscosities. The Shen *et al.* (2001) model specifies a simple Newtonian viscous rheology that is horizontally homogeneous in the crust, but incorporates a weak zone within the deep crust of the plateau above a much stronger mantle. Because no equivalent to the Greater Himalayan Sequence crops out on the eastern margin of Tibet, there is no equivalently detailed geohistory to be matched by more complex models. The style of flow in these two models is certainly consistent

with that inferred from the mid-crustal radial anisotropy measured from surface waves (Shapiro *et al.* 2004). Given the large body of evidence for the extreme weakness of the middle and lower crust and upper mantle north of the Banggong–Nujiang suture, the greater part of the strength of the lithosphere surely resides in the upper crust. The upper crust is deforming in a nearly continuous strain field (at least when measured at scales of *c.* 100 km; Chen *et al.* 2004; Zhang *et al.* 2004), and this eastward expulsion of Tibetan upper crust between India and Tarim/Qaidam suggests an additional top-driven Couette component to the mid-lower crustal flow. Conversely, the surface velocity field is far more continuous than the mid-crustal flow directions inferred by Clark & Royden (2000) from the topographic slopes of the eastern margin of Tibet (NE-directed north of the Sichuan Basin and SE-directed to the south with no or low flow predicted eastwards beneath the Sichuan Basin; Fig. 8), implying at least some decoupling of flow at different depths in the lithosphere. Rather than the upper crust completely driving upper-mantle deformation (Flesch *et al.* 2005), to some extent the upper mantle may be deforming independently, though fortuitously in a seemingly vertically coherent fashion because of the imposition of near-identical boundary conditions (Holt 2000).

Summary

The now extensive geophysical measurements in Tibet, catalogued above, imply temperatures and rheologies that require crustal flow. Crustal seismic velocities are so low and crustal attenuation so high that Tibetan crust is surely fluid-rich, a conclusion also demanded by the MT data. Great crustal thickness requires temperatures above the pelitic wet solidus even in areas of low heat flow, as is also suggested for Tibet by recent magmatic activity, so that many of these crustal fluids are likely to be partial melts. These fluids weaken the middle and lower crust as shown by the low elastic thickness, low topographic relief and shallow cut-off to crustal seismicity on the Tibetan Plateau. These geophysical measurements represent actual conditions; hence Tibetan crust today is hot, fluid-rich and weak. Though strong crustal anisotropy and reflectivity do not require active deformation, most plausibly they are diagnostic of ongoing flow in today's weak crust.

My assessment of specific modes of crustal flow should be considered more tenuous and likely to be changed in significant ways by future modelling and data acquisition. Nonetheless, Indian underthrusting in southern Tibet is most consistent with a south-directed flow of the middle crust with respect to both the Tibetan upper crust and Indian lower crust/upper mantle – conceptually a Poiseuille-type flow. No geophysical evidence requires the very explicit formulation of the channel-flow model by Beaumont *et al.* (2004) and Jamieson *et al.* (2004) for southern Tibet, but all the geophysical data are consistent with it – inevitably, since the model was designed *a posteriori* to fit the observations. Some geological data (Robinson & Pearson 2006; Harrison 2006) disagree with specific predictions of the preferred Beaumont *et al.* (2004) model, but it seems probable that the model could be tuned further to match these observations also. In northern and eastern Tibet, flow patterns are still less certain, in large part because of uncertainty about the strength of the mantle lithosphere. A reasonable assessment of sometimes conflicting datasets suggests there may be a weakly coupled flow of less viscous mid-lower crust above more viscous mantle lithosphere, involving elements of both Poiseuille- and Couette-type flow. The current generation of coupled thermal–mechanical models is 2D, but will need to become 3D in order to simultaneously model the clearly different rheological stratification (Fig. 7), hence inferred different flow patterns (Fig. 8), in different parts of Tibet. Meanwhile, field geophysicists need to acquire new transects across the plateau to broaden the perspective gained by intense focus on the most logistically accessible corridor across eastern Tibet, on which most models for the development of Tibet and the Himalaya are based.

I was privileged to work on the INDEPTH transect under the leadership of Doug Nelson from 1992 until his untimely death in 2002. Doug and my other INDEPTH colleagues provided my education about Tibet. I also thank those vocal participants at the Channel Flow conference who made me better informed about competing models and challenges to the INDEPTH paradigm of channel flow in southern Tibet. R. Bendick significantly improved my understanding of flow modelling through her review; additional reviews provided by M. Searle and R. Law, and comments and access to preprints from P. DeCelles, P. Kapp, J. Ni, L. Flesch, D. Grujic, C. Beaumont, M. Edwards, M. Harrison, K. Hodges, R. A. Jamieson, D. Robinson, C. Ruppel and A. Sheehan all contributed to making this a better and more comprehensive paper. The INDEPTH transect is funded by the NSF Continental Dynamics Program.

References

AFONSO, J. C. & RANALLI, G. 2004. Crustal and mantle strengths in continental lithosphere: is the jelly sandwich model obsolete? *Tectonophysics*, **394**, 221–232.

ALSDORF, D. & NELSON, D. 1999. Tibetan satellite magnetic low; evidence for widespread melt in the Tibetan crust? *Geology*, **27**, 943–946.

ALSDORF, D., BROWN, L., NELSON, K. D., MAKOVSKY, Y., KLEMPERER, S. L. & ZHAO, W.-J. 1998*a*. Crustal deformation of the Lhasa terrane, Tibet plateau from INDEPTH deep seismic reflection profiles. *Tectonics*, **17**, 501–519.

ALSDORF, D., MAKOVSKY, Y., ZHAO, W.-J. *ET AL.* 1998*b*. INDEPTH (International Deep Profiling of Tibet and the Himalaya) multi-channel seismic reflection data: Description and availability. *Journal of Geophysical Research*, **103**, 26,993–26,999.

AMMON, C. J., RANDALL, G. E. & ZANDT, G. 1990. On the nonuniqueness of receiver function inversions. *Journal of Geophysical Research*, **95**, 15,303–15,318.

AVOUAC, J.-P. 2003. Mountain building, erosion, and the seismic cycle in the Nepal Himalaya. *Advances in Geophysics*, **46**, 1–80.

BAILEY, R. C. 1990 Trapping of aqueous fluids in the deep crust. *Geophysical Research Letters*, **17**, 1129–1132.

BARAZANGI, M. & NI, J. 1982. Velocities and propagation characteristics of Pn and Sn beneath the Himalayan arc and Tibetan plateau; possible evidence for underthrusting of Indian continental lithosphere beneath Tibet. *Geology*, **10**, 179–185.

BEAUMONT C., JAMIESON, R. A., NGUYEN, M. H. & MEDVEDEV, S. 2004. Crustal channel flows: 1. Numerical models with applications to the tectonics of the Himalayan-Tibetan orogen. *Journal of Geophysical Research*, **109**, B06406. DOI: 10.1029/2003JB002809.

BEAUMONT C., NGUYEN, M. H., JAMIESON, R. A. & ELLIS, S. 2006. Crustal flow modes in large hot orogens. *In*: LAW, R. D., SEARLE, M. P. & GODIN, L. (eds) *Channel Flow, Ductile Extrusion and Exhumation in Continental Collision Zones*. Geological Society, London, Special Publications, **268**, 91–145.

BEGHOUL, N., BARAZANGI, M. & ISACKS, B. L. 1993. Lithospheric structure of Tibet and western North America; mechanisms of uplift and a comparative study. *Journal of Geophysical Research*, **98**, 1997–2016.

BENDICK, R. 2004. Topography associated with flow over an indenter in a rigid deformable channel (abstract). *In*: SEARLE, M. P., LAW, R. D. & GODIN, L. (convenors) Programme and abstracts for conference on: *Channel Flow, Ductile Extrusion and Exhumation of Lower-Mid Crust in Continental Collision Zones*, 6–7 December 2004, Geological Society, London.

BIRD, P. 1991. Lateral extrusion of lower crust from under high topography, in the isostatic limit. *Journal of Geophysical Research*, **96**, 10,275–10,286.

BRACE, W. F. & KOHLSTEDT, D. L. 1980. Limits on lithospheric stress imposed by laboratory experiments. *Journal of Geophysical Research*, **85**, 6248–6252.

BRAITENBERG, C., WANG, Y., FANG, J. & HSU, H. 2003. Spatial variations of flexure parameters over the Tibet–Quinghai plateau. *Earth and Planetary Science Letters*, **205**, 211–224.

BRANDON, C. & ROMANOWICZ, B. 1986. A "no-lid" zone in the center Chang-Thang platform of Tibet: Evidence from pure path phase velocity measurements of long period Rayleigh waves. *Journal of Geophysical Research*, **91**, 6547–6564.

BROWN, L. D., ZHAO, W., NELSON, K. D. *ET AL.* 1996. Bright spots, structure and magmatism in southern Tibet from INDEPTH seismic reflection profiling. *Science*, **274**, 1688–1690.

BURCHFIEL, B. C. & ROYDEN, L. H. 1985. North-south extension within the convergent Himalayan region. *Geology*, **13**, 679–682.

BUROV, E. B. & WATTS, A. B. 2006. The long-term strength of continental lithosphere: 'jelly sandwich' or 'crème brûlée'. *GSA Today*, **16**(1), 4–10.

CATTIN, R., MARTELET, G., HENRY, P., AVOUAC, J. P., DIAMENT, M. & SHAKYA, T. R. 2001. Gravity anomalies, crustal structure and thermo-mechanical support of the Himalaya of central Nepal. *Geophysical Journal International*, **147**, 381–392.

CHEN, L., BOOKER, J., JONES, A., NONG, W., UNSWORTH, M., WEI, W. & TAN, H. 1996. Electromagnetic images of colliding continents: A magnetotelluric survey of the Tsangpo Suture Zone and surrounding regions. *Science*, **274**, 1694–1696.

CHEN, Q., FREYMUELLER, J., WANG, Q., YANG, Z., XU, C. & LIU, J. 2004. A deforming block model for the present day tectonics of Tibet. *Journal of Geophysical Research*, **109**, B01403. DOI: 10.1029/2002JB002151.

CHEN, W.-P. & MOLNAR, P. 1983. Focal depths of intracontinental and intraplate earthquakes and their implications for the thermal and mechanical properties of the lithosphere. *Journal of Geophysical Research*, **88**, 4183–4214.

CHEN, W.-P. & ÖZALAYBEY, S. 1998. Correlation between seismic anisotropy and Bouguer gravity anomalies in Tibet and its implications for lithospheric structures. *Geophysical Journal International*, **135**, 93–101.

CHEN, W.-P. & YANG, Z. H. 2004. Earthquakes beneath the Himalayas and Tibet; evidence for strong lithospheric mantle. *Science*, **304**, 1949–1952.

CHRISTENSEN, N. I. 1996. Poisson's ratio and crustal seismology. *Journal of Geophysical Research*, **101**, 3139–3156.

CHRISTENSEN, N. I. & MOONEY, W. D. 1995. Seismic velocity structure and composition of the continental crust; a global view. *Journal of Geophysical Research*, **100**, 9761–9788.

CHUN, K.-Y. & YOSHII, T. 1977. Crustal structure of the Tibetan Plateau; a surface-wave study by a moving window analysis. *Bulletin of the Seismological Society of America*, **67**, 735–750.

CHUNG, S.-L., LIU, D.-Y., JI, J.-Q. *ET AL.* 2003. Adakites from continental collision zones: melting of thickened lower crust beneath southern Tibet. *Geology*, **31**, 1021–1024.

CLARK, M. K. & ROYDEN, L. H. 2000. Topographic ooze; building the eastern margin of Tibet by lower crustal flow. *Geology*, **28**, 703–706.

CLARK, M. K., SCHOENBOHM, L. M., ROYDEN, L. H., *ET AL.* 2004. Surface uplift, tectonics, and erosion

of eastern Tibet from large-scale drainage patterns. *Tectonics*, **23**, TC1006. DOI:10.1029/2002TC001402.

CLARK, M. K., BUSH, J. W. M. & ROYDEN, L. H. 2005. Dynamic topography produced by lower crustal flow against rheological strength heterogeneities bordering the Tibetan Plateau. *Geophysical Journal International*, **162**, 575–590.

COGAN, M. J., NELSON, K. D., KIDD, W. S. F. & WU, C. 1998. Shallow structure of the Yadong-Gulu rift, southern Tibet, from refraction analysis of Project INDEPTH common midpoint data. *Tectonics*, **17**, 46–61.

COTTE, N., PEDERSEN, H., CAMPILLO, M., MARS, J, NI, J. F., KIND, R., SANDVOL, E. & ZHAO, W. 1999. Determination of the crustal structure in southern Tibet by dispersion and amplitude analysis of Rayleigh waves. *Geophysical Journal International*, **138**, 809–819.

D'ANDREA, J., HARRISON, T. M., GROVE, M. & LIN, D. 2001. The thermal evolution of the Nyainqentanglha Shan; evidence for a long-lived, lower crustal magmatic system in southern Tibet. *Journal of Asian Earth Sciences*, **19**, 12–13.

DAVIS, P., ENGLAND, P. & HOUSEMAN, G. 1997. Comparison of shear wave splitting and finite strain from the India-Asia collision zone. *Journal of Geophysical Research*, **102**, 27,511–27,522.

DECELLES P. G., ROBINSON, D. M. & ZANDT, G. 2002. Implications of shortening in the Himalayan fold-thrust belt for uplift of the Tibetan Plateau. *Tectonics*, **21**(6), 1062. DOI: 10.1029/2001TC001322.

DEWEY, J. F. & BURKE, K. C. 1973. Tibetan, Variscan, and Precambrian basement reactivation: products of continental collision. *Journal of Geology*, **81**, 683–692.

DING, L., KAPP, P., ZHONG, D. & DENG, W. 2003. Cenozoic volcanism in Tibet: evidence for a transition from oceanic to continental subduction. *Journal of Petrology*, **44**, 1833–1865.

DRICKER I. G. & ROECKER, S. W. 2002. Lateral heterogeneity in the upper mantle beneath the Tibetan plateau and its surroundings from SS-S travel time residuals. *Journal of Geophysical Research*, **107**, 2305. DOI: 10.1029/2001JB000797.

ENGLAND, P. C. & HOUSEMAN, G. A. 1986. Finite strain calculations of continental deformation; 2, Comparison with the India-Asia collision zone. *Journal of Geophysical Research*, **91**, 3664–3676.

ENGLAND, P. & MOLNAR, P. 1997. Active deformation of Asia: From kinematics to dynamics. *Science*, **278**, 647–650.

FAN, G.-W. & LAY, T. 2002. Characteristics of Lg attenuation in the Tibetan Plateau. *Journal of Geophysical Research*, **107**, 2256. DOI: 10.1029/2001JB000804.

FAN, G.-W. & LAY, T. 2003. Strong Lg attenuation in the Tibetan Plateau. *Bulletin of the Seismological Society of America*, **93**, 2264–2272.

FIELDING, E., ISACKS, B., BARAZANGI, M. & DUNCAN, C. C. 1994. How flat is Tibet? *Geology*, **22**, 163–167.

FLESCH, L. M., HOLT, W. E., SILVER, P. G., STEPHENSON, M., WANG, C.-Y. & CHAN, W. W. 2005. Constraining the extent of crust-mantle coupling in central Asia using GPS, geologic, and shear-wave splitting data. *Earth and Planetary Science Letters*, **238**, 248–268.

FRANCHETEAU, J., JAUPART, C., SHEN, X. J., KANG, W. H., LEE, D. L., BAI, J. C., WEI, H. P. & DENG, H. Y. 1984. High heat flow in southern Tibet. *Nature*, **307**, 32–36.

FREDERIKSEN, A. W., FOLSOM, H. & ZANDT, G. 2003. Neighbourhood inversion of teleseismic Ps conversions for anisotropy and layer dip. *Geophysical Journal International*, **155**, 200–212.

GAILLARD, F., SCAILLET, B. & PICHAVANT, M. 2004. Evidence for present-day leucogranite pluton growth in Tibet, *Geology*, **32**, 801–804.

GALVÉ, A., HIRN, A., JIANG, M. *ET AL.* 2002*a*. Modes of raising northeastern Tibet probed by explosion seismology. *Earth and Planetary Science Letters*, **203**, 35–43.

GALVÉ, A., SAPIN, M., HIRN, A., DIAZ, J., LÉPINE, J.-C., LAIGLE, M., GALLART, J. & JIANG, M. 2002*b*. Complex images of Moho and variation of Vp/Vs across the Himalaya and South Tibet, from a joint receiver-function and wide-angle-reflection approach. *Geophysical Research Letters*, **29**, 2182. DOI: 10.1029/2002GL015611.

GALY, A. & FRANCE-LANORD, C. 2001. Higher erosion rates in the Himalaya; geochemical constraints on riverine fluxes. *Geology*, **29**, 23–26.

GAO, R., HUANG, D., LU, D. *ET AL.* 2000. Deep seismic reflection profile across the juncture zone between the Tarim Basin and the West Kunlun Mountains. *Chinese Science Bulletin*, **45**, 2281–2286.

GOES S. & VAN DER LEE, S. 2002. Thermal structure of the North American uppermost mantle inferred from seismic tomography. *Journal of Geophysical Research*, **107**. DOI: 10.1029/2000JB000049.

GOKARN, S. G., GUPTA, G., RAO, C. K. & SELVARAJ, C. 2002. Electrical structure across the Indus Tsangpo suture and Shyok suture zones in NW Himalaya using magnetotelluric studies. *Geophysical Research Letters*, **29**, 1–4.

GRASEMANN, B. & VANNAY, J.-C. 1999. Flow controlled inverted metamorphism in shear zones. *Journal of Structural Geology*, **21**, 743–750.

GREEN, A. G., MILKEREIT, B., PERCIVAL, J. A. *ET AL.* 1990. Origin of deep crustal reflections; seismic profiling across high-grade metamorphic terranes in Canada. *Tectonophysics*, **173**, 627–638.

GRUJIC, D., CASEY, M., DAVIDSON, C., HOLLISTER, L. S., KÜNDIG, R., PAVLIS, T. & SCHMID, S. 1996. Ductile extrusion of the Higher Himalayan Crystalline in Bhutan: evidence from quartz microfabrics, *Tectonophysics*, **260**, 21–43.

GRUJIC, D., HOLLISTER, L. S. & PARRISH, R. R. 2002. Himalayan metamorphic sequence as an orogenic channel; insight from Bhutan. *Earth and Planetary Science Letters*, **198**, 177–191.

GUPTA, M. L., SHARMA, S. R., DROLIA, R. K. & SINGH, S. B. 1983. Subsurface thermal conditions of Puga Valley hydrothermal field, Himalaya, India. *Journal of Geophysics*, **54**, 51–59.

HACKER, B. R., GNOS, E., RATSCHBACHER, L., GROVE, M., MCWILLIAMS, M., SOBOLEV, S. V.,

WAN, J. & WU, Z. 2000. Hot and dry deep crustal xenoliths from Tibet. *Science*, **287**, 2463–2466.

HAINES, S., KLEMPERER, S. L., BROWN, L. *ET AL.* 2003. Crustal thickening processes in central Tibet: implications of INDEPTH III seismic data. *Tectonics*, **22**, 1–18.

HAMMOND, W. C. & HUMPHREYS, E. D. 2000. Upper mantle seismic wave velocity: Effects of realistic partial melt geometries. *Journal of Geophysical Research*, **105**, 10,975–10,986.

HARINARAYANA, T., AZEEZ, K. K. A., NAGANJANEYULU, K., MANOJ, C., VEERASWAMY, K., MURTHY, D. N. & RAO, S. P. E. 2004. Magnetotelluric studies in Puga valley geothermal field, NW Himalaya, Jammu and Kashmir, India. *Journal of Volcanology and Geothermal Research*, **138**, 405–424.

HARRISON, T. M. 2006. Did the Himalayan Crystallines extrude from beneath the Tibetan Plateau? *In*: LAW, R. D., SEARLE, M. P. & GODIN, L. (eds) *Channel Flow, Ductile Extrusion and Exhumation in Continental Collision Zones.* Geological Society, London, Special Publications, **268**, 237–254.

HAUCK, M. L., NELSON, K. D., BROWN, L. D., ZHAO, W. J. & ROSS, A. R. 1998. Crustal structure of the Himalayan Orogen from Project INDEPTH deep seismic reflection profiles at *c.* 90°E. *Tectonics*, **17**, 481–500.

HENRY, P., LE PICHON, X. & GOFFE, B. 1997. Kinematic, thermal and petrological model of the Himalayas; constraints related to metamorphism within the underthrust Indian crust and topographic elevation. *Tectonophysics*, **273**, 31–56.

HERQUEL, G. & TAPPONNIER, P. 2005. Seismic anisotropy in western Tibet. *Geophysical Research Letters*, **32**, L17306. DOI: 10.1029/2005GL023561.

HERQUEL, G., WITTLINGER, G. & GUILBERT, J. 1995. Anisotropy and crustal thickness of Northern-Tibet. New constraints for tectonic modeling. *Geophysical Research Letters*, **22**, 1925–1928.

HILLEY G. E., BÜRGMANN, R., ZHANG, P.-Z. & MOLNAR, P. 2005. Bayesian inference of plastosphere viscosities near the Kunlun Fault, northern Tibet. *Geophysical Research Letters*, **32**, L01302. DOI: 10.1029/2004GL021658.

HIRN, A., LEPINE, J.-C., JOBERT, G. *ET AL.* 1984*a*. Crustal structure and variability of the Himalayan border of Tibet. *Nature*, **307**, 23–25.

HIRN, A., NERCESSIAN, A., SAPIN, M., JOBERT, G., XU Z. X., GAO E. Y., LU, D. Y. & TENG, J. W. 1984b. Lhasa Block and bordering sutures; a continuation of a 500-km Moho traverse through Tibet. *Nature*, **307**, 25–27.

HIRN, A., JIANG, M, SAPIN, M. *ET AL.* 1995. Seismic anisotropy as an indicator of mantle flow beneath the Himalayas and Tibet. *Nature*, **375**, 571–574.

HOCHSTEIN, M. P. & REGENAUER-LIEB, K. 1998. Heat generation associated with collision of two plates; the Himalayan geothermal belt. *Journal of Volcanology and Geothermal Research*, **83**, 75–92.

HODGES, K. V. 2006. The channel tunneling–extrusion hypothesis as developed for the Himalayan–Tibetan orogenic system. *In*: LAW, R. D., SEARLE, M. P. & GODIN, L. (eds) *Channel Flow, Ductile Extrusion and Exhumation in Continental Collision Zones*. Geological Society, London, Special Publications, **268**, 71–90.

HODGES, K. V., HURTADO, J. M. & WHIPPLE, K. X. 2001. Southward extrusion of Tibetan crust and its effect on Himalayan tectonics. *Tectonics*, **20**, 799–809.

HOKE, L., LAMB, S., HILTON, D. R. & POREDA, R. J. 2000. Southern limit of mantle-derived geothermal helium emissions in Tibet; implications for lithospheric structure. *Earth and Planetary Science Letters*, **180**, 297–308.

HOLBROOK, W. S., CATCHINGS, R. D. & JARCHOW, C. M. 1991. Origin of deep crustal reflections: implications of coincident seismic refraction and reflection data in Nevada. *Geology*, **19**, 175–179.

HOLNESS, M. B. 1993. Temperature and pressure dependence of quartz-aqueous fluid dihedral angles: the control of adsorbed H_2O on the permeability of quartzites. *Earth and Planetary Science Letters*, **117**, 363–377.

HOLT, W. E. 2000. Correlated crust and mantle strain fields in Tibet. *Geology*, **28**, 67–70.

HUANG, W.-C., NI, J. F., TILMANN, F. *ET AL.* 2000. Seismic polarization anisotropy beneath the central Tibetan Plateau. *Journal of Geophysical Research*, **105**, 27,979–27,990.

HUERTA A. D., ROYDEN L. H. & HODGES K. V. 1998. The thermal structure of collisional orogens as a response to accretion, erosion, and radiogenic heating. *Journal of Geophysical Research*, **103**, 15,287–15,302.

HURTADO, J. M., JR., HODGES, K. V. & WHIPPLE, K. 2001. Neotectonics of the Thakkhola Graben and implications for Recent activity on the South Tibetan fault system in the central Nepal Himalaya. *Geological Society of America Bulletin*, **113**, 222–240.

HYNDMAN, R. D. & SHEARER, P. M. 1989. Water in the lower continental crust; modelling magnetotelluric and seismic reflection results, *Geophysical Journal of the Royal Astronomical Society*, **98**, 343–365.

JACKSON, J. 2003. Faulting, flow and the strength of the continental lithosphere. *In*: KLEMPERER, S. L. & ERNST, W. G. (eds) *The George A. Thompson Volume: The Lithosphere of Western North America and its Geophysical Characterization.* Geological Society of America, International Book Series, **7**, 5–27.

JAMIESON R. A., BEAUMONT, C., MEDVEDEV, S. & NGUYEN, M. H. 2004. Crustal channel flows: 2. Numerical models with implications for metamorphism in the Himalayan-Tibetan orogen. *Journal of Geophysical Research*, **109**, B06407. DOI: 10.1029/2003JB002811.

JAMIESON, R. A., BEAUMONT, C., NGUYEN, M. H. & GRUJIC, D. 2006. Provenance of the Greater Himalayan Sequence and associated rocks: predictions of channel flow models. *In*: LAW, R. D., SEARLE, M. P. & GODIN, L. (eds) *Channel Flow, Ductile Extrusion And Exhumation In Continental*

Collision Zones. Geological Society, London, Special Publications, **268**, 165–182.

JAUPART, C., FRANCHETEAU, J. & SHEN, X.-J. 1985. On the thermal structure of the southern Tibetan crust. *Geophysical Journal of the Royal Astronomical Society*, **81**, 131–155.

JIN, Y., MCNUTT, M. K. & ZHU, Y. 1996. Mapping the descent of Indian and Eurasian plates beneath the Tibetan plateau from gravity anomalies. *Journal of Geophysical Research*, **101**, 11,275–11,290.

JOHNSON, M. R. W. 1994. Volume balance of erosional loss and sediment deposition related to Himalayan uplifts. *Journal of the Geological Society, London*, **151**, 217–220.

JONES, A. G. 1992. Electrical conductivity of the continental lower crust. *In*: FOUNTAIN, D. M., ARCULUS, R. & KAY, R. W. (eds) *Continental Lower Crust*. Elsevier, Amsterdam, 81–143.

JORDAN, T. A. & WATTS, A. B. 2005. Gravity anomalies, flexure and the elastic thickness structure of the India–Eurasia collisional system. *Earth and Planetary Science Letters*, **236**, 732–750.

KAO, H., GAO, R., RAU, R.-J., SHI, D., CHEN, R.-Y., GUAN, T. & WU, F. T. 2001. Seismic image of the Tarim basin and its collision with Tibet. *Geology*, **29**, 575–578.

KAPP, P. & GUYNN, J. H. 2004. Indian punch rifts Tibet. *Geology*, **32**, 993–996.

KAPP, J. L. D., HARRISON, T. M., KAPP, P., GROVE, M., LOVERA, O. M. & DING, L. 2005. Nyainqentanghla Shan: a window into the tectonic, thermal and geochemical evolution of the Lhasa block, southern Tibet. *Journal of Geophysical Research*, **110**, B08413. DOI: 10.1029/2004JB003330.

KIND, R., NI, J., ZHAO, W., WU, J. *ET AL.* 1996. Evidence from earthquake data for a partially molten crustal layer in Southern Tibet. *Science*, **274**, 1692–1694.

KIND, R., YUAN, X, SAUL, J. *ET AL.* 2002. Seismic images of crust and upper mantle beneath Tibet; evidence for Eurasian Plate subduction. *Science*, **298**, 1219–1221.

KING, J., HARRIS, N., ARGLES, T. & PARRISH, R. 2005. Constraints on tectonic models from crustal melt formation in southern Tibet. *In*: MASCLE, G. & LAVÉ, J. (eds) 20th Himalaya-Karakoram-Tibet Workshop Special Extended Abstracts Volume. *Géologie Alpine Mémoire H.S.* **44**, 104–105.

KIRBY, S. H. 1984. Introduction and digest to the special issue on chemical effects of water on the deformation and strengths of rocks. *Journal of Geophysical Research*, **89**, 3991–3995.

KLEMPERER, S. L. 1987. A relation between continental heat flow and the seismic reflectivity of the lower crust. *Journal of Geophysics*, **61**, 1–11.

KOLA-OJO, O. & MEISSNER, R. 2001. Southern Tibet; its deep seismic structure and some tectonic implications. *Journal of Asian Earth Sciences*, **19**, 249–256.

KONG, X., WANG, Q. & XIONG, S. 1996. Comprehensive geophysics and lithospheric structure in the western Xizang (Tibet) Plateau. *Science in China (Series D)*, **39**, 348–358.

KOONS, P. O., ZEITLER, P. K., CHAMBERLAIN, C. P., CRAW, D. & MELTZER, A. S. 2002. Mechanical links between erosion and metamorphism in Nanga Parbat, Pakistan Himalaya. *American Journal of Science*, **302**, 749–773.

KOSAREV, G., KIND, R., SOBOLEV, S. V., YUAN, X., HANKA, W. & ORESHIN, S. 1999. Seismic evidence for a detached Indian lithospheric mantle beneath Tibet. *Science*, **283**, 1306–1309.

KUMAR, P., YUAN, X., KIND, R. & NI, J. 2006. Imaging the colliding Indian and Asia lithospheric plates beneath Tibet. *Journal of Geophysical Research*, **111**, B06308. DOI: 10.1029/2005JB003930.

KUSZNIR, N. J. & MATTHEWS, D. H. 1988. Deep seismic reflections and the deformational mechanics of the continental lithosphere. *In*: MENZIES, M. A. & COX, K. G. (eds) Oceanic and continental lithosphere; similarities and differences. *Journal of Petrology*, Special Lithosphere issue, 63–87.

LACHENBRUCH, A. H. & SASS, J. H. 1977. Heat flow in the United States and the thermal regime of the crust. *In*: HEACOCK, J. G., KELLER, G. V., OLIVER, J. E. & SIMMONS, G. (eds) *The Earth's Crust; its Nature and Physical Properties*. American Geophysical Union, Geophysical Monographs, **20**, 626–675.

LANGIN, W. R., BROWN, L. D. & SANDVOL, E. A. 2003. Seismicity of central Tibet from Project INDEPTH III seismic recordings. *Bulletin of the Seismological Society of America*, **93**, 2146–2159.

LAVÉ, J., AVOUAC, J. P., LACASSIN, R., TAPPONNIER, P. & MONTAGNER, J. P. 1996. Seismic anisotropy beneath Tibet: evidence for eastward extrusion of the Tibetan lithosphere? *Earth and Planetary Science Letters*, **140**, 83–96.

LEE, J., HACKER, B. & WANG, Y. 2004. Evolution of North Himalayan gneiss domes: structural and metamorphic studies in Mabja dome, southern Tibet. *Journal of Structural Geology*, **26**, 2297–2316.

LEECH, M. L., SINGH, S., JAIN, A. K., KLEMPERER, S. L. &. MANICKAVASAGAM, R. M. 2005. The onset of India–Asia continental collision: Early, steep subduction required by the timing of UHP metamorphism in the western Himalaya. *Earth and Planetary Science Letters*, **234**, 83–97

LEMONNIER, C., MARQUIS, G., PERRIER, F. *ET AL.* 1999. Electrical structure of the Himalaya of Central Nepal: high conductivity around the mid-crustal ramp along the MHT. *Geophysical Research Letters*, **26**, 3261–3264.

LI, J., MILLER, B. V., NELSON, K. D. & SAMSON, S. D. 1998. Two belts of collisional granite in the Himalaya? *EOS Transactions of the American Geophysical Union*, **79**, Suppl., 350.

LI, S., UNSWORTH, M. J., BOOKER, J. R., WEI W., TAN H. & JONES, A. G. 2003. Partial melt or aqueous fluid in the mid-crust of southern Tibet? Constraints from INDEPTH magnetotelluric data. *Geophysical Journal International*, **153**, 289–304.

MCKENZIE, D. & FAIRHEAD, D. 1997. Estimates of the effective elastic thickness of the continental lithosphere from Bouguer and free air gravity

anomalies. *Journal of Geophysical Research*, **102**, 27,523–27,552.

McKENZIE, D. & JACKSON, J. 2002. Conditions for flow in the continental crust. *Tectonics*, **21**(6), 1055. DOI: 10.1029/2002TC001394.

McKENZIE, D., NIMMO, F., JACKSON, J. A., GANS, P. B. & MILLER, E. L. 2000. Characteristics and consequences of flow in the lower crust. *Journal of Geophysical Research*, **105**, 11,029–11,046.

McNAMARA, D. E., OWENS, T. J., SILVER, P. G. & WU, F. T. 1994. Shear wave anisotropy beneath the Tibetan Plateau. *Journal of Geophysical Research*, **99**, 13,655–13,666.

McNAMARA, D. E., OWENS, T. J. & WALTER, W. R. 1995. Observation of regional phase propagation across the Tibetan Plateau. *Journal of Geophysical Research*, **100**, 22,215–22,229.

McNAMARA, D. E., WALTER, W. R., OWENS, T. J. & AMMON, C. J. 1997. Upper mantle velocity structure beneath the Tibetan plateau from Pn travel time tomography. *Journal of Geophysical Research*, **102**, 493–505.

MAGGI, A., JACKSON, J. A., PRIESTLEY, K. & BAKER, C. 2000. A reassessment of focal depth distributions in southern Iran, the Tien Shan and northern India: Do earthquakes really occur in the continental mantle? *Geophysical Journal International*, **143**, 629–661.

MAKOVSKY, Y. & KLEMPERER, S. L. 1999. Measuring the seismic properties of Tibetan bright spots: Evidence for free aqueous fluids in the Tibetan middle crust. *Journal of Geophysical Research*, **104**, 10,795–10,825.

MAKOVSKY, Y., KLEMPERER, S. L., HUANG, L.-Y. LU, D.-Y. & PROJECT INDEPTH TEAM. 1996. Structural elements of the southern Tethyan Himalaya crust from wide-angle seismic data. *Tectonics*, **15**, 997–1005.

MAKOVSKY, Y., KLEMPERER, S. L., RATSCHBACHER, L. & ALSDORF, D. 1999. Midcrustal reflector on INDEPTH wide-angle profiles: An ophiolitic slab beneath the India-Asia suture in southern Tibet? *Tectonics*, **18**, 793–808.

MALTHE-SØRENSSEN, A., PLANKE, S., SVENSEN, H. & JAMTVEIT, B. 2004. Formation of saucer-shaped sills. *In*: BREITKREUZ, C. & PETFORD, N. (eds) *Physical Geology of High-Level Magmatic Systems*. Geological Society, London, Special Publications, **234**, 215–227.

MASEK, J. G., ISACKS, B. L., FIELDING, E. J. & BROWAEYS, J. 1994. Rift flank uplift in Tibet; evidence for a viscous lower crust. *Tectonics*, **13**, 659–667.

MECHIE, J., SOBOLEV, S. V., RATSCHBACHER, L. *ET AL.* 2004. Precise temperature estimation in the Tibetan crust from seismic detection of the alpha-beta quartz transition. *Geology*, **32**, 601–604.

MEDVEDEV, S. & BEAUMONT, C. 2006. Growth of continental plateaus by channel injection: models designed to address constraints and thermomechanical consistency. *In*: LAW, R. D., SEARLE, M. P. & GODIN, L. (eds) *Channel Flow, Ductile Extrusion and Exhumation in Continental Collision Zones*. Geological Society, London, Special Publications, **268**, 147–164.

MEISSNER, R. & STREHLAU, J. 1982. Limits of stresses in continental crusts and their relation to the depth-frequency distribution of shallow earthquakes. *Tectonics*, **1**, 73–89.

MELTZER, A., SARKER, G., BEAUDOIN, B., SEEBER, L. & ARMBRUSTER, J. 2001. Seismic characterization of an active metamorphic massif, Nanga Parbat, Pakistan Himalaya. *Geology*, **29**, 651–654.

MIBE, K., FUJII, T. & YASUDA, A. 1999. Control of the location of the volcanic front in island arcs by aqueous fluid connectivity in the mantle wedge. *Nature*, **401**, 259–262.

MITRA, S., PRIESTLEY, K., BHATTACHARYYA, A. K. & GAUR, V. K. 2005. Crustal structure and earthquake focal depths beneath northeastern India and southern Tibet. *Geophysical Journal International*, **160**, 227–248.

MOLNAR, P. 1988. A review of geophysical constraints on the deep structure of the Tibetan Plateau, the Himalaya and the Karakoram, and their tectonic implications. *Philosophical Transactions of the Royal Society of London, Series A*, **326**, 33–88.

MOLNAR, P. 2000. Large-Scale Continental Dynamics. *In: Abstracts of the Second Plate Boundary Observatory (PBO) Workshop*, Palm Springs, California, 30 October–1 November 2000. (www.scec.org/news/01news/es_abstracts/molnar.pdf).

MOLNAR, P. & CHEN, W.-P. 1983. Focal depths and fault plane solutions of earthquakes under the Tibetan Plateau. *Journal of Geophysical Research*, **88**, 1180–1196.

MOLNAR, P. & LYON-CAEN, H. 1989. Fault plane solutions of earthquakes and active tectonics of the Tibetan plateau and its margins. *Geophysical Journal of the Royal Astronomical Society*, **99**, 123–153.

MOLNAR, P., ENGLAND, P. & MARTINOD, J. 1993. Mantle dynamics, uplift of the Tibetan Plateau, and the Indian monsoon. *Reviews of Geophysics*, **31**, 357–396.

MONSALVE, G., SHEEHAN, A. F., SCHULTE-PECKUM, V., RAJAURE, S., PANDEY, M. R. & WU, F. 2006. Seismicity and 1-D velocity structure of the Himalayan collision zone: earthquakes in the crust and upper mantle. *Journal of Geophysical Research* (in press).

MYROW, P. M., HUGHES, N. C., PAULSEN, T. S. *ET AL.* 2003. Integrated tectonostratigraphic analysis of the Himalaya and implications for its reconstruction. *Earth Planetary Science Letters*, **212**, 433–441.

NELSON, K. D., ZHAO, W., BROWN, L. D. *ET AL.* 1996. Partially molten middle crust beneath southern Tibet; synthesis of Project INDEPTH results. *Science*, **274**, 1684–1688.

NI, J. & BARAZANGI, M. 1983. High-frequency seismic wave propagation beneath the Indian Shield, Himalayan Arc, Tibetan plateau and surrounding regions; high uppermost mantle velocities and efficient Sn propagation beneath Tibet. *Geophysical Journal of the Royal Astronomical Society*, **72**, 665–689.

OWENS, T. J. & ZANDT, G. 1997. Implications of crustal property variations for models of Tibetan plateau evolution. *Nature*, **387**, 37–43.

OZACAR, A. A. & ZANDT, G. 2004. Crustal seismic anisotropy in central Tibet: Implications for deformational style and flow in the crust. *Geophysical Research Letters*, **31**, L23601. DOI: 10.1029/2004GL021096.

PATINO DOUCE, A. & HARRIS, N. 1998. Experimental constraints on Himalayan anatexis. *Journal of Petrology*, **39**, 689–710.

PHAM, V. N., BOYER, D., THERME, P., YUAN, X. C., LI, L. & JIN, G. Y. 1986. Partial melting zones in the crust in southern Tibet from magnetotelluric results. *Nature*, **319**, 310–314.

PRIESTLEY, K. & MCKENZIE, D. 2006. The thermal structure of the lithosphere from shear wave velocities. *Earth and Planetary Science Letters*, **244**, 285–301.

RAI, S. S., PRIESTLEY, K., GAUR, V. K., SINGH, M. P. & SEARLE, M. 2006. Configuration of the Indian Moho beneath the NW Himalaya and Ladakh. *Geophysical Research Letters*, **33**, L15308. DOI: 10.1029/2006GL026076.

RANDALL, G. E., AMMON, C. J. & OWENS, T. J. 1995. Moment-tensor estimation using regional seismograms from portable network deployments. *Geophysical Research Letters*, **22**, 1665–1668.

RAPINE R., TILMANN, F., WEST, M., NI, J. & RODGERS, A. 2003. Crustal structure of northern and southern Tibet from surface wave dispersion analysis. *Journal of Geophysical Research*, **108**, 2120. DOI: 10.1029/2001JB000445.

ROBINSON, D. M. & PEARSON, O. N. 2006. Exhumation of Greater Himalayan rocks along the Main Central Thrust in Nepal: implications for channel flow. *In*: LAW, R. D., SEARLE, M. P. & GODIN, L. (eds) *Channel Flow, Ductile Extrusion and Exhumation in Continental Collision Zones*. Geological Society, London, Special Publications, **268**, 255–267.

RODGERS, A. J. & SCHWARTZ, S. Y. 1998. Lithospheric structure of the Qiangtang Terrane, northern Tibetan Plateau, from complete regional waveform modeling: Evidence for partial melt. *Journal of Geophysical Research*, **103**, 7137–7152.

ROSENBERG, C. L. & HANDY, M. R. 2005. Experimental deformation of partially melted granite revisited; implications for the continental crust. *Journal of Metamorphic Geology*, **23**, 19–28.

ROSS, A. R., BROWN, L. D., PANANONT, P., NELSON, K. D., KLEMPERER, S. L., HAINES, S., ZHAO, W. & GUO, J. 2004. Deep reflection surveying in central Tibet: lower-crustal layering and crustal flow. *Geophysical Journal International*, **156**, 115–128.

ROYDEN, L. H. 1996. Coupling and decoupling of crust and mantle in convergent orogens; implications for strain partitioning in the crust. *Journal of Geophysical Research*, **101**, 17,679–17,705.

ROYDEN, L. H., BURCHFIEL, B. C., KING, R. W., WANG, E., CHEN Z., SHEN F. & LIU Y. 1997. Surface deformation and lower crustal flow in eastern Tibet. *Science*, **276**, 788–790.

RUPPEL, C. & MCNAMARA, D. E. 1997. Seismic and rheological constraints on the thermal state of Tibetan plateau upper mantle: implications for melt production, mantle delamination and large-scale tectonics. *EOS Transactions of the American Geophysical Union*, **78**, 650.

RUZAIKIN, A. I., NERSESOV, I. L., KHALTURIN, V. I. & MOLNAR, P. 1977. Propagation of Lg and lateral variations in crustal structure in Asia. *Journal of Geophysical Research*, **82**, 307–316.

SANDVOL, E., NI, J., KIND, R. & ZHAO, W. 1997. Seismic anisotropy beneath the southern Himalayas–Tibet collision zone. *Journal of Geophysical Research*, **102**, 17,813–17,824.

SAPIN, M. & HIRN, A. 1997. Seismic structure and evidence for eclogitization during the Himalayan convergence. *Tectonophysics*, **273**, 1–16.

SCHULTE-PELKUM, V., GASPAR, M., SHEEHAN, A., PANDEY, M. R., SAPKOTA, S., BILHAM, R. & WU, F. 2005. Imaging the Indian subcontinent beneath the Himalaya. *Nature*, **435**, 1222–1225. DOI: 10.1038/nature03678.

SEARLE, M. P. & REX, A. J. 1989. Thermal model for the Zanskar Himalaya. *Journal of Metamorphic Geology*, **7**, 127–134.

SEARLE, M. P. & SZULC, A. G. 2005. Channel flow and ductile extrusion of the High Himalayan slab – the Kangchenjunga–Darjeeling profile, Sikkim Himalaya. *Journal of Asian Earth Sciences*, **25**, 173–185.

SHANKER, R., PADHI, R. N., ARORA, C. L., PRAKASH, G., THUSSU, J. L & DUA, K. J. S. 1976. Geothermal exploration of the Puga and Chumathang geothermal fields, Ladakh, India. *In*: *Proceedings, Second United Nations Symposium on the Development and Use of Geothermal Resources*, San Francisco, USA, 20–29 May 1975. US Government Printing Office, Washington DC, **1**, 245–258.

SHAPIRO, N. M., RITZWOLLER, M. H., MOLNAR, P. & LEVIN, V. 2004. Thinning and flow of Tibetan crust constrained by seismic anisotropy. *Science*, **305**, 233–236.

SHEN, F., ROYDEN, L. H. & BURCHFIEL, B. C. 2001. Large-scale crustal deformation of the Tibetan Plateau. *Journal of Geophysical Research*, **106**, 6793–6816.

SHERRINGTON, H. F., ZANDT, G. & FREDERIKSEN, A. 2004. Crustal fabric in the Tibetan plateau based on waveform inversions for seismic anisotropy parameters. *Journal of Geophysical Research*, **109**, B02312. DOI: 10.1029/2002JB002345.

SHI, D, ZHAO, W., BROWN, L. *ET AL*. 2004. Detection of southward intra-continental subduction of Tibetan lithosphere along the Bangong-Nujiang suture by P-to-S converted waves. *Geology*, **32**, 209–212.

SILVER, P. G. 1996. Seismic anisotropy beneath the continents: probing the depths of geology. *Annual Reviews of Earth and Planetary Science*, **24**, 385–432.

SPRATT, J. E., JONES, A. G., NELSON, K. D., UNSWORTH, M. J. & INDEPTH MT TEAM. 2005. Crustal structure of the India–Asia collision zone, southern Tibet, from INDEPTH MT investigations. *Physics of the Earth and Planetary Interiors*, **150**, 227–237.

TAPPONNIER, P., PELTZER, G., LEDAIN, A. Y., ARMIJO, R. & COBBOLD, P. 1982. Propagating extrusion tectonics in Asia–new insights from simple experiments with plasticine, *Geology* **10**, 611–616.

TAPPONNIER, P., XU, Z. Q., ROGER, F., MEYER, B., ARNAUD, N., WITTLINGER, G. & YANG, J. S. 2001. Oblique stepwise rise and growth of the Tibet plateau. *Science* **294**, 1671–1677.

TAYLOR, M., YIN, A., RYERSON, F. J., KAPP, P. & DING, L. 2003. Conjugate strike-slip faulting along the Bangong–Nujiang suture zone accommodates coeval east–west extension and north–south shortening in the interior of the Tibetan Plateau. *Tectonics*, **22**(4), 1044. DOI: 10.1029/2002TC001361.

THOMPSON, A. B. & CONNOLLY, J. A. D. 1995. Melting of the continental crust: Some thermal and petrological constraints on anatexis in continental collision zones and other tectonics settings. *Journal of Geophysical Research*, **100**, 15,565–15,579.

THOMSON, K. 2004. Sill complex geometry and internal architecture: A 3D seismic perspective. *In*: BREITKREUZ, C. & PETFORD, N. (eds) *Physical Geology of High-Level Magmatic Systems*. Geological Society, London, Special Publications, **234**, 229–232.

TIAN, X., WU, Q., ZHANG, Z., TENG, J. & ZENG, R. 2005. Joint imaging by teleseimic converted and multiple waves and its applications in the INDEPTH-III passive seismic array. *Geophysical Research Letters*, **32**, L21315. DOI: 10.1029/2005GL023686.

TIKOFF, B., RUSSO, R., TEYSSIER, C. & TOMMASI, A. 2004. Mantle-driven deformation of orogenic zones and clutch tectonics. *In*: GROCOTT, J., MCCAFFREY, K. J. W., TAYLOR, G. & TIKOFF, B. (eds) *Vertical Coupling and Decoupling in the Lithosphere*. Geological Society, London, Special Publications, **227**, 41–64.

TILMANN, F., NI, J. & INDEPTH III SEISMIC TEAM. 2003. Seismic imaging of the downwelling Indian lithosphere beneath central Tibet. *Science*, **300**, 1424–1427.

TORAMARU, A. & FUJII, N. 1986. Connectivity of melt phase in a partially molten peridotite. *Journal of Geophysical Research*, **91**, 9239–9252.

TURNER, S., ARNAUD, N., LIU, J. *ET AL.* 1996. Post-collision, shoshonitic volcanism on the Tibetan Plateau; implications for convective thinning of the lithosphere and the source of ocean island basalts. *Journal of Petrology*, **37**, 45–71.

UNSWORTH, M., WEI W., JONES, A. G. *ET AL.* 2004. Crustal and upper mantle structure of northern Tibet imaged with magnetotelluric data. *Journal of Geophysical Research*, **109**, B02403. DOI: 10.1029/2002JB002305.

UNSWORTH, M. J., JONES, A. G., WEI W., MARQUIS, G., GOKARN, S. G., SPRATT, J. E. & THE INDEPTH-MT TEAM. 2005. Crustal rheology of the Himalaya and Southern Tibet inferred from magnetotelluric data. *Nature*, **483**, 78–81. DOI: 10.1038/nature04154.

VERGNE, J., WITTLINGER, G., QIANG H., TAPPONNIER, P., POUPINET, G., JIANG M., HERQUEL, G. & PAUL, A. 2002. Seismic evidence for stepwise thickening of the crust across the NE Tibetan Plateau. *Earth and Planetary Science Letters*, **203**, 25–33.

VERGNE J., WITTLINGER, G., FARRA, V. & SU, H. 2003. Evidence for upper crustal anisotropy in the Songpan-Ganze (northeastern Tibet) terrane. *Geophysical Research Letters*, **30**. DOI: 10.1029/2002GL016847.

WAFF, H. S. & BULAU, J. R. 1979. Equilibrium fluid distribution in an ultramafic partial melt under hydrostatic stress conditions. *Journal of Geophysical Research*, **84**, 6109–6114.

WANG Q., ZHANG P., FREYMUELLER, J. T. *ET AL.* 2001. Present-day crustal deformation in China constrained by Global Positioning System measurements. *Science*, **294**, 574–577.

WANG, Q., MCDERMOTT, F., XU, J.-F., HERVÉ BELLON, H. & ZHU, Y.-T. 2005. Cenozoic K-rich adakitic volcanic rocks in the Hohxil area, northern Tibet: Lower-crustal melting in an intracontinental setting. *Geology*, **33**, 465–468.

WANG, Y. 2001. Heat flow pattern and lateral variations of lithosphere strength in China mainland; constraints on active deformation. *Physics of the Earth and Planetary Interiors*, **126**, 121–146.

WARNER, M. R. 1990. Basalts, water, or shear zones in the lower continental crust? *Tectonophysics*, **173**, 163–174.

WATSON, E. B. & LUPULESCU, A. 1993. Aqueous fluid connectivity and chemical transport in clinopyroxene-rich rocks. *Earth and Planetary Science Letters*, **117**, 279–294.

WEI, W., UNSWORTH, M., JONES, A. *ET AL.* 2001. Detection of widespread fluids in the Tibetan crust by magnetotelluric studies. *Science*, **292**, 716–718.

WILLETT, S. D. 1999. Orogeny and orography: The effects of erosion on the structure of mountain belts. *Journal of Geophysical Research*, **104**, 28,957–28,982.

WILLETT, S. D. & BEAUMONT, C. 1994. Subduction of Asian lithospheric mantle beneath Tibet inferred from models of continental collision. *Nature*, **369**, 642–645.

WILLIAMS, H. M., TURNER, S. P., PEARCE, J. A., KELLEY, S. P. & HARRIS, N. B. W. 2004. Nature of the source regions for post-collisional, potassic magmatism in southern and northern Tibet from geochemical variations and inverse trace element modelling. *Journal of Petrology*, **45**, 555–607.

WITTLINGER, G., MASSON, F., POUPINET, G. *ET AL.* 1996. Seismic tomography of northern Tibet and Kunlun; evidence for crustal blocks and mantle velocity contrasts. *Earth and Planetary Science Letters*, **139**, 263–279.

WITTLINGER, G., TAPPONNIER, P., POUPINET, G., MEI, J., SHI, D., HERQUEL, G. & MASSON, F. 1998. Tomographic evidence for localized lithospheric shear along the Altyn Tagh Fault. *Science*, **281**, 74–76.

WITTLINGER, G., VERGNE, J., TAPPONNIER, P. *ET AL.* 2004. Teleseismic imaging of subducting lithosphere and Moho offsets beneath western Tibet. *Earth and Planetary Science Letters*, **221**, 117–130.

WOBUS, C. W. HODGES, K. V. & WHIPPLE, K. X. 2003. Has focused denudation sustained active thrusting at the Himalayan topographic front? *Geology*, **31**, 861–864.

WU, C., NELSON, K. D., WORTMAN, G., SAMSON, S. D., YUE, Y., LI, J., KIDD, W. S. F. & EDWARDS, M. A. 1998. Yadong cross structure and South Tibetan Detachment in the east central Himalaya (89°–90°E). *Tectonics*, **17**, 28–45. DOI: 10.1029/97TC03386.

XIE, J., GOK, R., NI, J. & AOKI, Y. 2004. Lateral variations of crustal seismic attenuation along the INDEPTH profiles in Tibet from Lg Q inversion. *Journal of Geophysical Research*, **109**, B10308. DOI: 10.1029/2004JB002988.

YOSHINO T., MIBE, K., YASUDA, A. & FUJII, T. 2002. Wetting properties of anorthite aggregates: Implications for fluid connectivity in continental lower crust. *Journal of Geophysical Research*, **107**. DOI: 10.1029/2001JB000440.

YUAN, X., NI, J., KIND, R., MECHIE, J. & SANDVOL, E. 1997. Lithospheric and upper mantle structure of southern Tibet from a seismological passive source experiment. *Journal of Geophysical Research*, **102**, 27,491–27,500.

ZEITLER, P. K., KOONS, P. O., BISHOP, M. P. *ET AL.* 2001. Crustal reworking at Nanga Parbat, Pakistan: Metamorphic consequences of thermal-mechanical coupling facilitated by erosion. *Tectonics*, **20**, 712–728. DOI: 10.1029/2000TC001243.

ZHANG, P.-Z., SHEN, Z., WANG, M. *ET AL.* 2004. Continuous deformation of the Tibetan plateau from global positioning system data. *Geology*, **32**, 809–812.

ZHANG, Z.-J. & KLEMPERER, S. L. 2005. West-east variation in crustal thickness in northern Lhasa block, central Tibet, from deep seismic sounding data. *Journal of Geophysical Research*, **110**, B09403. DOI: 10.1029/2004JB003139.

ZHAO, J., MOONEY, W. D., ZHANG, X., LI, Z., JIN, Z. & OKAYA, N. 2006. Crustal structure across the Altyn Tagh Range at the northern margin of the Tibetan plateau and tectonic implications. *Earth and Planetary Science Letters*, **241**, 804–814.

ZHAO, L. S. & HELMBERGER, D. V. 1991. Geophysical implications from relocations of Tibetan earthquakes; hot lithosphere. *Geophysical Research Letters*, **18**, 2205–2208.

ZHAO, L. S., SEN, M. K., STOFFA, P. & FROHLICH, C. 1996. Application of very fast simulated annealing to the determination of the crustal structure beneath Tibet. *Geophysical Journal International*, **125**, 355–370.

ZHAO, W.-J., NELSON, K. D. & PROJECT INDEPTH TEAM. 1993. Deep seismic reflection evidence for continental underthrusting beneath southern Tibet. *Nature*, **366**, 557–559.

ZHAO, W., MECHIE, J., BROWN, L. D. *ET AL.* J. 2001. Crustal structure of central Tibet as derived from project INDEPTH wide-angle seismic data. *Geophysical Journal International*, **145**, 486–498.

ZHAO, W.-L. & MORGAN, W. J. 1987. Injection of Indian crust into Tibetan lower crust: A two-dimensional finite element model study. *Tectonics*, **6**, 489–504.

ZHU, L. & HELMBERGER, D. V. 1996. Intermediate depth earthquakes beneath the India–Tibet collision zone. *Geophysical Research Letters*, **23**, 435–438.

ZHU, L. & HELMBERGER, D. V. 1998. Moho offset across the northern margin of the Tibetan Plateau. *Science*, **281**, 1170–1172.

ZOBACK, M. D., TOWNEND, J. & GROLLIMUND, B. 2003. Steady-state failure equilibrium and deformation of intraplate lithosphere. *In*: KLEMPERER, S. L. & ERNST, W. G. (eds) *The George A. Thompson Volume: The Lithosphere of Western North America and its Geophysical Characterization.* Geological Society of America, International Book Series, **7**, 50–68.